European Journal of Medicinal Chemistry 123 (2016) 649–664

Contents lists available at ScienceDirect

European Journal of Medicinal Chemistry

journal homepage: http://www.elsevier.com/locate/ejmech

Research paper

X-ray crystal structures of *Enterococcus faecalis* thymidylate synthase with folate binding site inhibitors

Alessia Catalano [a, 1], Rosaria Luciani [b, 1], Alessia Carocci [a], Debora Cortesi [b], Cecilia Pozzi [c], Chiara Borsari [b], Stefania Ferrari [b, **], Stefano Mangani [c, *]

[a] Dipartimento di Farmacia-Scienze del Farmaco, Università degli Studi di Bari "Aldo Moro", Via Orabona 4, 70125 Bari, Italy
[b] Dipartimento di Scienze della Vita, Università degli Studi di Modena e Reggio Emilia, Via Campi 103, 41125 Modena, Italy
[c] Dipartimento di Biotecnologie, Chimica e Farmacia, Università degli Studi di Siena, Via Aldo Moro 2, 53100 Siena, Italy

ARTICLE INFO

Article history:
Received 26 April 2016
Received in revised form
25 July 2016
Accepted 26 July 2016
Available online 29 July 2016

Keywords:
Enterococcus faecalis
Enzyme inhibition
Thymidylate synthase
X-ray crystallography screening
Phthalimide scaffold
Antibacterial

ABSTRACT

Infections caused by *Enterococcus faecalis* (*Ef*) represent nowadays a relevant health problem. We selected Thymidylate synthase (TS) from this organism as a potential specific target for antibacterial therapy. We have previously demonstrated that species-specific inhibition of the protein can be achieved despite the relatively high structural similarity among bacterial TSs and human TS. We had previously obtained the *Ef*TS crystal structure of the protein in complex with the metabolite 5-formyl-tetrahydrofolate (5-FTHF) suggesting the protein role as metabolite reservoir; however, protein–inhibitors complexes were still missing. In the present work we identified some inhibitors bearing the phthalimidic core from our in-house library and we performed crystallographic screening towards *Ef*TS. We obtained two X-ray crystallographic structures: the first with a weak phthalimidic inhibitor bound in one subunit and 5-hydroxymethylene-6-hydrofolic acid (5-HMHF) in the other subunit; a second X-ray structure complex with methotrexate. The structural information achieved confirm the role of *Ef*TS as an enzyme involved in the folate pool system and provide a structural basis for structure-based drug design.

1. Introduction

Enterococci can be found in soil, food and water and make up a significant portion of the normal gut flora of humans and animals. As for other bacteria of the gut flora, *enterococci* can also cause infectious diseases. Typical enterococcal infections occur in immunosuppressed patients and in hospitalized patients suffering from a wide spectrum of severe illnesses. *Enterococci* nowadays rank second to third in frequency among bacteria isolated from hospitalized patients. They can be often isolated from urinary tract infections, intra-abdominal and pelvic infections, bacteremias, wounds, tissue infections and endocarditis as part of a polymicrobial flora. *Enterococcus faecalis* (*Ef*) and *Enterococcus faecium* are the most prevalent species cultured from humans and they are present in more than 90% of clinical isolates. *Enterococcus faecalis* accounts for 80–90% of clinical strains, while *Enterococcus faecium* for only 5–10%. Some strains of *E. faecalis* and many of *E. faecium* are resistant to multiple antimicrobials [1]. The identification of new antibiotics targeting *Enterococci* infections is challenging since no specific antibacterial agents are known so far. This encourages the starting of active drug discovery programs. Molecules targeting the *Enterococci* folate pathway represent a source of potential and specific drugs able to inhibit the bacterial folate pathway without altering, in principle, the mammalian cells. In our antibacterial discovery programs we have identified some lead compounds bearing a phthalimide moiety targeting bacterial *Lactobacillus casei* (*Lc*) and *Escherichia coli* (*Ec*) thymidylate synthase (TS) and able to discriminate between the bacterial and the host (human) protein. This selectivity led to the discovery of antibacterial agents with a low toxicity [2–10]. TS (EC: 2.1.1.45) catalyzes the reductive methylation of 2′-deoxyuridine-5′-monophosphate (dUMP) to 2′-deoxythymidine-5′-monophosphate (dTMP), assisted by the cofactor N^5,N^{10}-methylene tetrahydrofolate (MTHF) [11,12]. TS is the only synthetic source of dTMP in human cells, thus it represents a major target for the design of chemotherapeutic agents [13]. The

* Corresponding author.
** Corresponding author.
E-mail addresses: stefania.ferrari@unimore.it (S. Ferrari), stefano.mangani@unisi.it (S. Mangani).
[1] Alessia Catalano and Rosaria Luciani contribute equally to the work. The work was written through contributions of all authors.

http://dx.doi.org/10.1016/j.ejmech.2016.07.066
0223-5234/

well-known anticancer agents, 5-fluorouracil (the prodrug of 5-fluoro-2′-deoxyuridine monophosphate), methotrexate (MTX) and raltitrexed (Fig. 1), are classical TS inhibitors belonging to the antimetabolite class. In our previous work, compound **α156** (Fig. 1) had been proposed as an antibacterial lead able to face vancomycin-resistant infections caused by gram positive bacteria such as *Staphylococcus aureus*. This molecule also inhibited the *Enterococcus faecalis* clinical isolates and showed a low toxicity towards human cells [7]. In a parallel work we had identified a library of phthalimidic derivatives, 4-methylisoindoline-1,3-dione *N*-derivatives (**I,** Fig. 1) and 4-(aminomethyl)-2-methylisoindoline-1,3-dione derivatives substituted at the amino position (**II**, Fig. 1), that presented inhibitory activity against bacterial TS enzymes. These phthalimidic derivatives inhibited also *Enterococcus faecalis* TS (*Ef*TS), with the best inhibitors showing K_i in the range of 2–8 μM. These compounds exhibited a competitive behavior with respect to the folate cofactor and a significant selectivity towards bacterial TS [8]. *Ef*TS X-ray crystal structure of the native protein had been obtained [14]. According to structural analysis, the protein crystallized in a ternary complex where a folate substrate analogue, 5-formyl-tetrahydrofolate (5-FTHF), originating from the bacterial metabolites pool, co-crystallized with the enzyme. Thus, we can conclude that *Ef*TS could be considered a reservoir for folate substrates in the bacteria folate dependent metabolism. Although no structural information about *Ef*TS-inhibitors complexes are available yet, we could suppose that the target druggability is influenced by the presence of the folate metabolites inside the bacterial cell and that higher affinity inhibitors are necessary to displace 5-FTHF. Aiming to obtain X-ray crystallographic structures to gain additional information on *Ef*TS target druggability and to carry out further structure-based drug design studies, we analyzed our in-house library based on a *N*-substituted phthalimide scaffold bearing a flexible chain linked to the nitrogen in position 2. In details, 56 compounds (Charts 1 and 2) were tested against *Ef*TS, *Ec*TS and human TS (hTS). In the present work, X-ray crystallographic screenings were carried out and one X-ray crystallography complex with a protein inhibitor, (*S*)-**12**, was obtained. In addition, we solved the X-ray crystal structure of *Ef*TS in complex with methotrexate (MTX), a known folate analogue. These studies represent an important starting point for a structure-based drug design aimed at identifying new antibacterial agents against *Enterococcus faecalis* infections.

2. Results and discussion

2.1. Library selection and compound synthesis

With the aim of exploring the chemical space of the phthalimide core, a library of 56 compounds (Charts 1 and 2) was selected from our in-house libraries (for details see experimental section), previously synthesized as intermediates for the preparation of compounds with different pharmacological activities [15–33]. These compounds underwent *in vitro* screening towards *Ef*TS, hTS and *Ec*TS. All the molecules of the new library show an *N*-substituted phthalimide ring (**III**, Fig. 1). The majority of the compounds have an aromatic ring in the side-chain linked to position 2 of the phthalimide moiety. In our previously published library the aromatic moiety in the side-chain was directly linked to the nitrogen in position 2 (**I**, Fig. 1), whereas in the present work almost all the compounds have a spacer between the phthalimide core and the aromatic system of the side-chain, thus being more flexible. Few compounds (**27**–**31, 34, 56**) have a non-aromatic side-chain with a lower steric hindrance. This novel phthalimide library includes several chiral compounds (**1**–**8, 12, 13, 17, 21, 27**–**34, 40**–**43, 50, 51, 56**) and for some of them we explored the biological profile of both the racemic mixture and the single enantiomers.

2.2. Chemistry

Only synthetic procedures followed to obtain compounds not previously characterized in literature are described in this paper. The synthesis of the racemic mixture and of the enantiomers of compound **8** is shown in Scheme 1. Ester (*RS*)-**60** was obtained following Williamson reaction of (*RS*)-bromopropanoate, (*RS*)-**58** with 2,6-dimethylphenol, while (*R*)- and (*S*)-**61** were obtained by Mitsunobu reaction [34,35] of 2,6-dimethylphenol with (*S*)- or (*R*)-methyl lactate [(*S*)- or (*R*)-**59**], respectively. After esters reduction, the obtained alcohols **61** were submitted to Mitsunobu reaction with phthalimide to give the desired compounds. Compound **13** was obtained through hydrolysis of compound **12** (Scheme 2). The synthesis of compounds (*S*)-**17,** (*S*)- and (*R*)-**33** is depicted in Scheme 3. (*S*)- and (*R*)-**33** were obtained by protecting (*S*)- and (*R*)-2-amino-2-phenylethanol, respectively, with phthalic anhydride. Iodination of compound (*S*)-**33** yielded compound (*S*)-**17**. Compounds **20** and **22** were synthesized as reported in Scheme 4. Cyano derivative **18** was converted into the corresponding trimethyltintetrazole derivative **62** by reaction with azido-trimethyltin. The treatment of compound **62** with gaseous HCl gave tetrazole derivative **22**, which was alkylated with methyl iodide to give compound **20**. Compound **24** was obtained by reacting 2-(methoxycarbonyl)benzoic acid with *p*-toluidine in presence of EEDQ as previously described (Scheme 5) [36]. The nitration of (*R*)-**63**, followed by reduction of the nitro group gave (*R*)-**7** and, successively, (*R*)-**43** (Scheme 6), as reported in the literature [26,37,38]. Compounds **25** and **55** were prepared by protecting 4-phenylbutan-1-amine with phthalimide or tetrachlorophthalimide, respectively (Scheme 7). The synthesis of compound **52** is reported in Scheme 8. 3-aminopropanol was protected with phthalic anhydride to give compound **64,** which was submitted to Mitsunobu reaction with 1-naphthol. Compound **65** (Scheme 9) was synthesized by the reaction of 3-aminopropanol with tetrachlorophthalic anhydride and converted into compound **53**. The synthesis of compound **54** is depicted in Scheme 10. Williamson reaction on 3-bromopropanol with thiophenol gave compound **67** which was converted into the thioether **55**. Finally, the synthesis of (*R*)-**1** was obtained via a Mitsunobu reaction starting from (*S*)-**68** (Scheme 11).

2.3. Biological evaluation of the compounds library

The selected 56 compounds were tested against *Ef*TS and hTS enzymes in order to evaluate the inhibitory activity towards TS and the specificity towards the bacterial enzyme (Fig. 2, Table S1, see Supplementary Material). The percentage of inhibition (I %) at 100 μM are reported as heat-map plot in Fig. 2 in which different color codes represent the inhibition range of the compounds. Moreover, the inhibitory activity towards *Escherichia coli* TS (*Ec*TS) was assessed, aiming to explore a larger biological activity profile. Several compounds of the library are chiral, thus they were tested as racemic mixture and/or as homochiral. Thirteen compounds (**4, 7, 11, 18, 20, 23, 35, 39, 40, 45, 47, 52** and **54**) show inhibitory activity towards *Ef*TS (I % = 20–60% at 100 μM). Compounds **18**, (*R*)-**40** and **54**, with K_i of 25, 13 and 24 μM, respectively, turned out to be the best inhibitors of the library. Moreover, they were species-specific inhibitors of *Ef*TS, since they were inactive at 100 μM towards hTS. Few compounds (*RS*)-**1**, (*R*)-**7**, (*R*)-**8**, **9**, **14**, **16**, **24, 25** were able to decrease the *Ec*TS activity by 35–48% at 100 μM and represent the most potent *Ec*TS inhibitors of this set of compounds. In our previous paper [8], we studied the inhibitory activity towards *Ef*TS of more rigid phthalimide derivatives (**6A**, **8A**, **12A**,

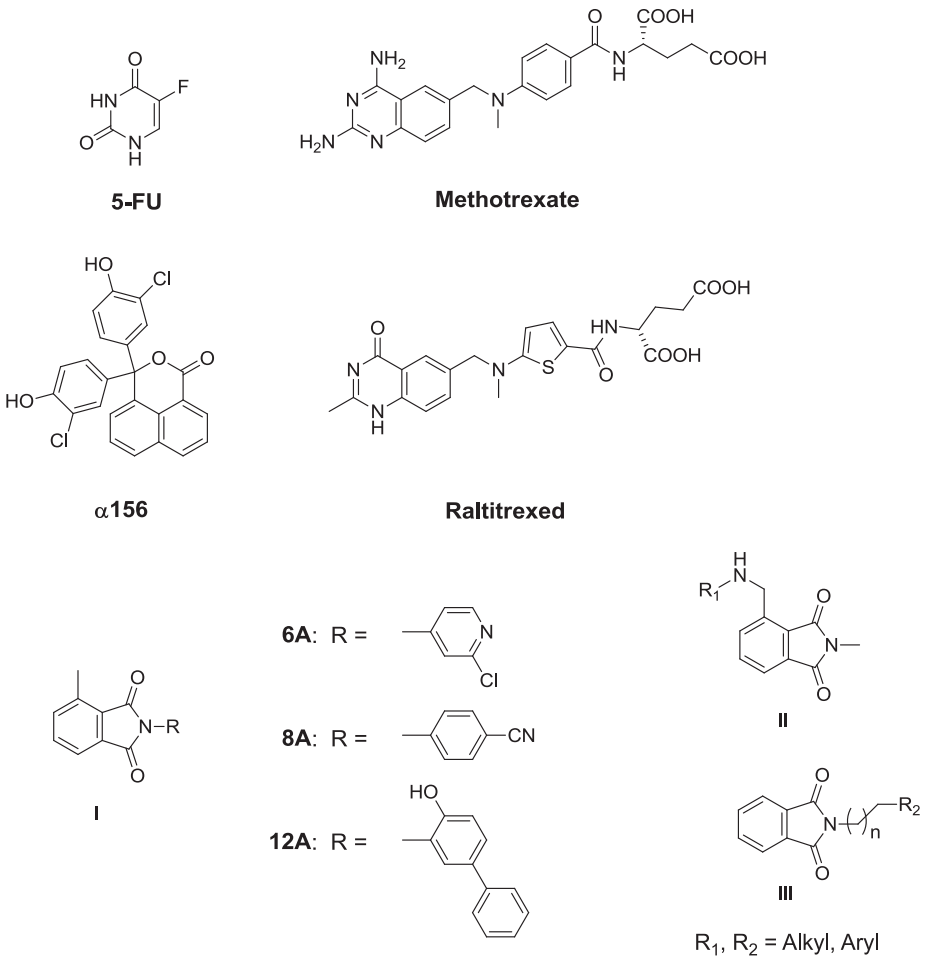

Fig. 1. Chemical structure of TS inhibitors and the prodrug 5FU.

Fig. 1). The phthalimide moiety had been directly connected to substituted aromatic or heteroaromatic rings in position 2. Compound **6A**, **8A** and **12A** showed a significant *Ef*TS inhibitory activity, with compound **12A** being the most active ($K_i = 2.0 \pm 0.35$ μM). In the present study, we evaluated the activity of more flexible molecules. The spacer between the phthalimide moiety and the aromatic side chain was from 2 to 10 carbons long (Fig. 1, III). In most cases, an ether or a thioether spacer was used. If we compare the overall inhibitory activity of the previously published library with that of the present library, we can state that more rigid compounds are preferable with respect to flexible molecules, for *Ef*TS binding.

2.4. X-ray crystal structures of EfTS in complex with (S)-12 and with MTX

X-ray crystallographic studies were carried out on structurally different N-substituted phthalimides. Overall, the present library showed medium to low affinity towards *Ef*TS. All the compounds showing a percentage of inhibition towards *Ef*TS of 10%–60% were selected for the crystallographic screening. From the screened crystals, we obtained usable diffraction data only for *Ef*TS complexes with (*R*)-**2**, (*S*)-**12** and **14**. Unfortunately, the Fourier difference maps for (*R*)-**2** and **14** complexes showed only blurred features corresponding to the bound inhibitor into the active site that prevented model building. In addition, we also obtained a dataset for *Ef*TS bound by MTX ($K_i = 13$ μM) that has been used for comparison. Eventually, only the electron density for the (*S*)-**12** inhibitor bound to *Ef*TS was complete and confidently interpreted (PDB: 4O7U) and compared with that of *Ef*TS-MTX complex (PDB: 5J7W). MTX has a K_i equal to that of the best phtalimidic inhibitor of the series, compound (*R*)-**40**. The two independent *Ef*TS dimers present in the crystal asymmetric unit of the *Ef*TS-(*S*)-**12** complex (Fig. 3A) display subunit heterogeneity: one subunit is empty and in the 'open' conformation [14], while the other one hosts the exogenous ligand and is in a 'closed' conformation (Fig. 3B). The 'open' conformation is characterized by the loop 92–102 being open and mostly disordered and by the short helix 103–109 and the first two turns of helix 111–130 being completely unfolded. In the 'closed' conformation the secondary structure elements described above are fully ordered with the loop closer to the active site cavity (see Fig. 3B). Further heterogeneity is present in the 'closed' subunits as they bind two different molecules into their active sites. We observed a mixture of two different complexes: 5-hydroxymethylene-6-hydrofolic acid (5-HMHF) is found in one dimer (Fig. 4A), while the other dimer hosts the *S*-enantiomer of compound (*RS*)-**12** used for co-crystallization (Fig. 4B). Subunit heterogeneity and half-site reactivity is commonly found in TS enzymes [39–41]. The electron density present in the active site of the B subunit led to identify the folate analogue as 5-hydroxymethylene-6-hydrofolate molecule (5-HMHF), thus different from the 5-formyltetrahydrofolate (5-FTHF) already published [14]. The active site cavity of the B subunit shows electron density above noise, which is consistent with the planar structure of the pteridine moiety and in contrast with the puckered pyrazine

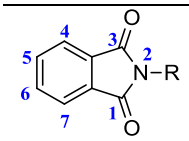

Compd	R	Compd	R	Compd	R
1	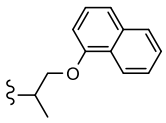	**2**	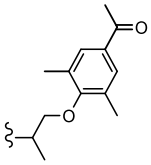	**3**	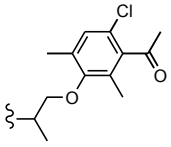
4	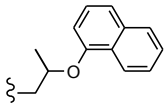	**5**	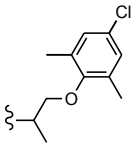	**6**	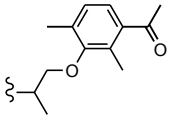
7	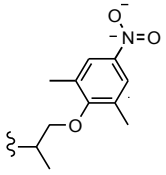	**8**	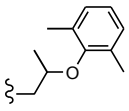	**9**	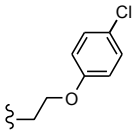
10	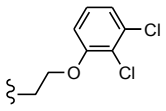	**11**	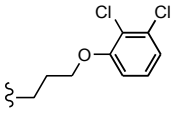	**12**	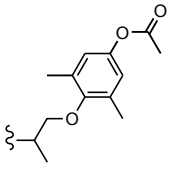
13	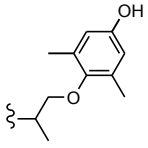	**14**	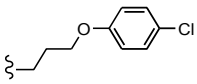	**15**	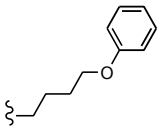

Chart 1. Compounds **1**–**52**.

ring of tetrahydrofolate found in our previous crystal structure of *Ef*TS [14] (Fig. 4A). The remaining parts of the molecule establish interactions similar to those of 5-FTHF. We have previously shown that *Ef*TS obtained from our preparations contains bound metabolites from the folate pathway, such as 5-formyl-tetrahydrofolate (5-FTHF; PDB: 3UWI) [14]. 5-HMHF is a product of the conversion of 5-FTHF by bacterial enzymes (e.g. 5,10-methenyl-tetrahydrofolate synthetase enzyme). In fact, 5-HMHF was discovered for the first time bound to 5,10-methenyl-tetrahydrofolate synthetase from *Mycoplasma pneumoniae* (PDB 1U3G) [42]. Analyzing the binding mode of (*S*)-**12**, we can suggest that this compound displaces 5-HMHF (or other folate structural analogues), at least partially, from *Ef*TS active site. This finding provides structural evidence of the competitive inhibition pattern of compound (*S*)-**12** with respect to MTHF. The orientation of compound (*S*)-**12** into *Ef*TS active site is similar to that of 5-FTHF and 5-HMHF (Fig. 4A–B). Compound (*S*)-**12** establishes interactions with the hydrophobic residues surrounding the active site (Ile80, Trp81, Trp84, Leu194, Cys197, Leu223, Phe227, Tyr260 and Ile313). Only one hydrogen bond between the carbonyl group of compound (*S*)-**12** and a water molecule is formed. The phthalimide core of compound (*S*)-**12** places itself in the same position occupied by the pteridine moiety of the 5-HMHF and the *para*-substituted aromatic chain replaces the PABA moiety of 5-HMHF. The phthalimide core is wrapped in a lipophilic binding site and interacts with Leu194, Trp84 and Trp81, typical residues involved in the cofactor binding. The aromatic side chain has contact distance from the side chains of Glu59 (3.4 Å), Trp84 (3.1 Å) and Phe227 (3.4 Å), while the acetoxy substituent in *para*

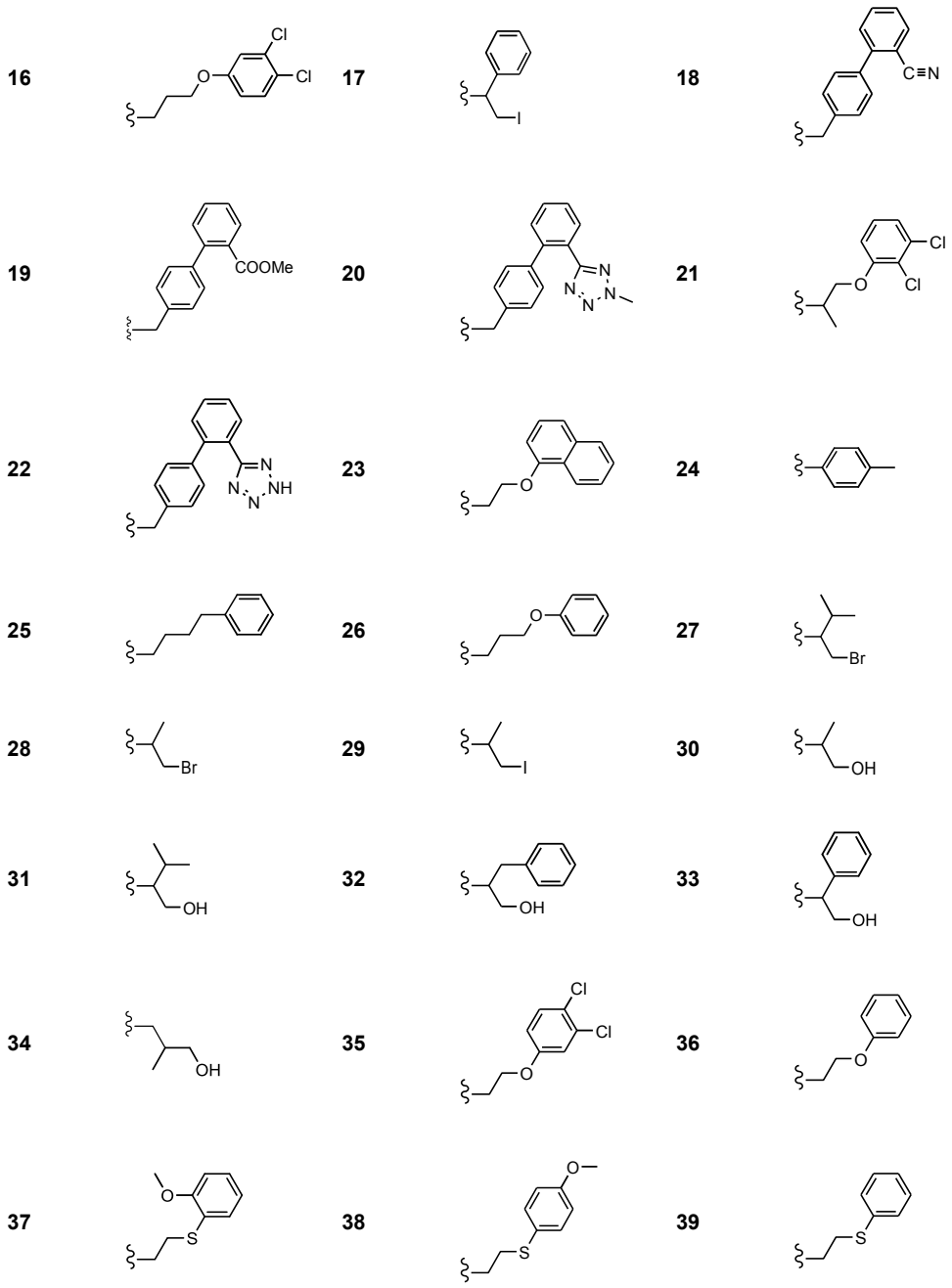

Chart 1. (*continued*).

position of the phenyl ring is at 3.7 Å from Leu223. In addition, the acetoxy group is located within 6.0–7.0 Å from several carbonyl groups of the main chain and from the backbone chains of Lys49 and Lys310. The absence of direct H-bonds and the prevalence of lipophilic interactions explain the low affinity of the compound for *Ef*TS. Compound (*S*)-**12** was the only compound of the series providing a crystal structure of its complex with *Ef*TS despite (*S*)-**12** is a weak inhibitor (10% at 100 μM). This occurs frequently when hits screenings are performed to identify X-ray crystal structures needed to start a structure-based drug design [43]. The puzzling aspect of our *Ef*TS is that, despite the addition of the dUMP to the crystallization medium, the substrate has never been found bound to the active site. A structural comparison between our enzyme and other bacterial TS that form ternary complexes with dUMP and folate analogues (e.g. PDB: 1NCE) [41,44] highlighted that 5-HMHF and (*S*)-**12** are bound closer to *Ef*TS catalytic Cys197 where usually dUMP binds, if compared to the folate analogues. However, a slight rearrangement of the cofactor could be expected to allow space for dUMP binding. Probably, the sulfate anions used at high concentration for crystallization compete for the same site where the phosphate group of dUMP binds [14]. Indeed, a sulfate anion is bound in the active site cavity at the same site in all subunits. This site corresponds to the binding site of the dUMP phosphate group in 1NCE as well as other *Escherichia. coli* TS complexes with dUMP

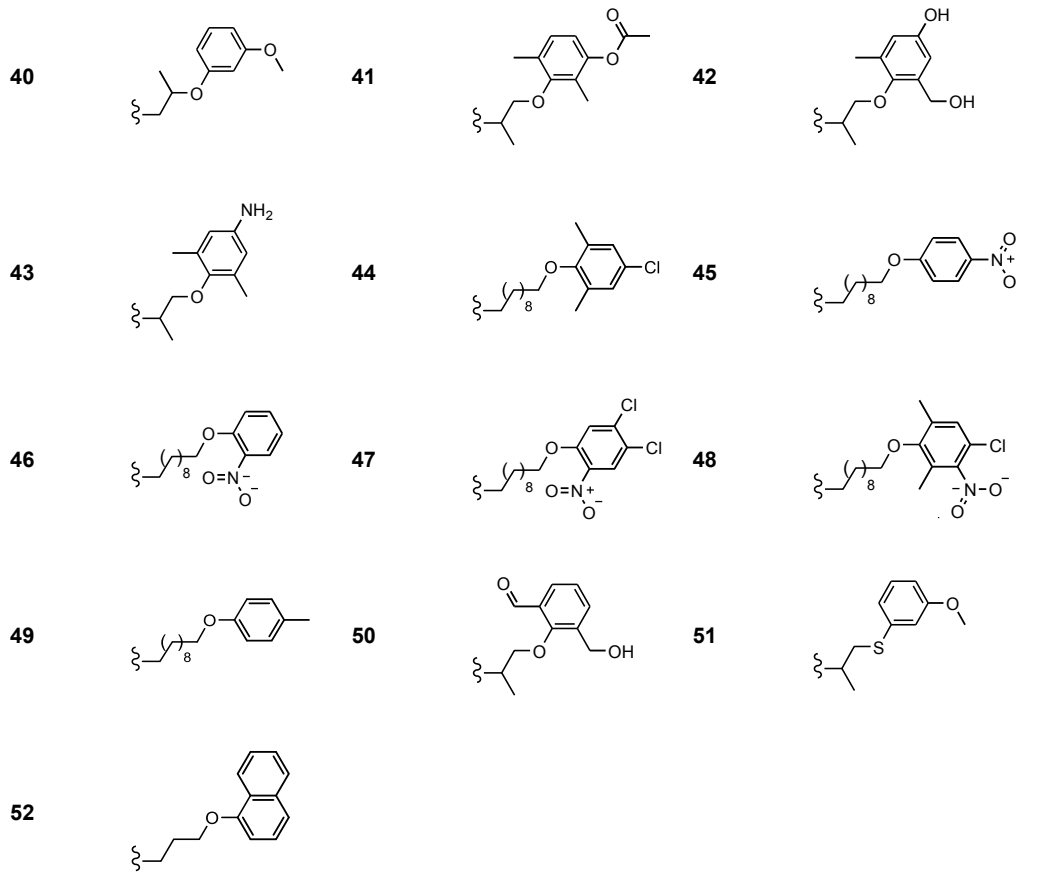

Chart 1. (*continued*).

Compd	Structure	Compd	Structure
53	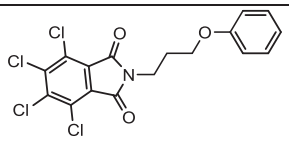	**54**	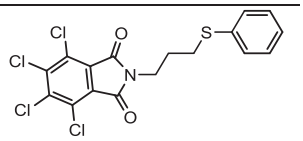
55	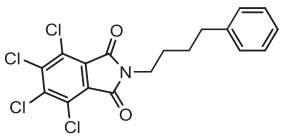	**56**	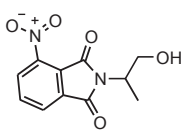

Chart 2. Compounds **53**–**56**.

and the inhibitors F9 (PDB: 4LRR) [10] or BGC 945 (PDB: 4ISK) [45,46]. In our previous paper [8] the crystallographic complexes of *Lc*TS with phthalimidic compounds (**I** in Fig. 1) have been obtained. Due to the structural similarity between *Lc*TS and *Ef*TS, we can compare the complexes of *Lc*TS-inhibitors already published [8] with the complex *Ef*TS-(*S*)-**12**. The compounds of the previously published library presented a phthalimide core directly linked to the side chain, thus they cannot assume a folded conformation and they show a binding mode different to that of compound (*S*)-**12**. Moreover, the presence of dUMP in *Lc*TS complexes suggested that dUMP induces a different orientation of the phtalimidic core into TS active site and contributes to stabilize the protein-ligand complex

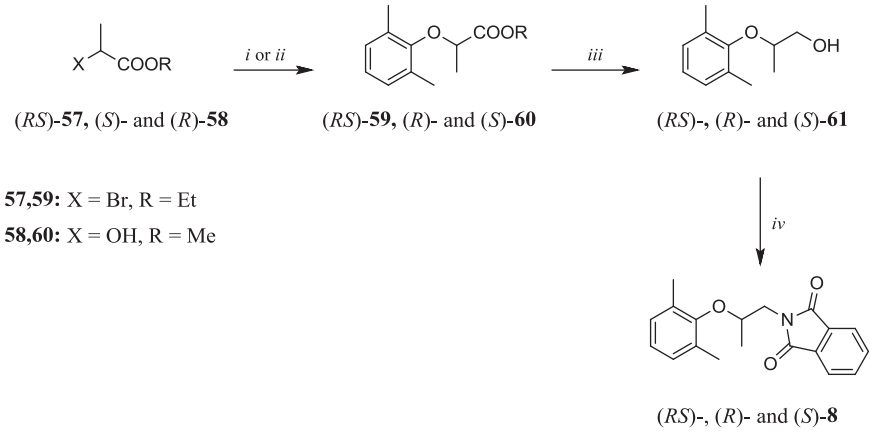

Scheme 1. Reagents and conditions: (i) 2,6-dimethyphenol, Na, abs EtOH, 70 °C, for (*RS*)-**59**; (ii) 2,6-dimethylphenol, PPh_3, DIAD, dry THF, rt, for (*R*)- and (*S*)-**60**; (iii) $LiAlH_4$, dry THF, reflux; (iv) phthalimide, PPh_3, DIAD, dry THF, rt.

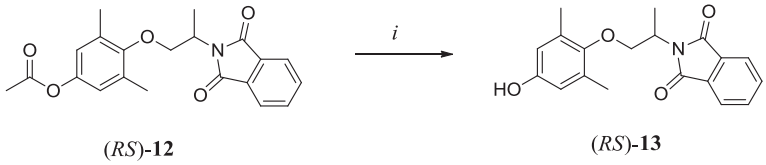

Scheme 2. Reagents and conditions: (i) 10% HCl, THF, 0 °C then rt.

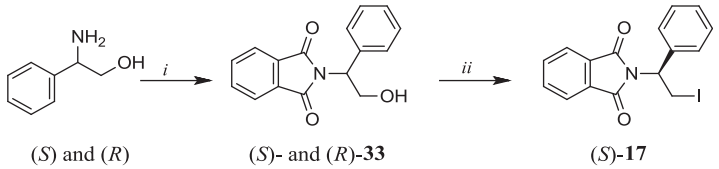

Scheme 3. Reagents and conditions: (i) phthalic anhydride, Et_3N, toluene, 130 °C; (ii) gaseous HI, dry toluene, −5 °C then rt.

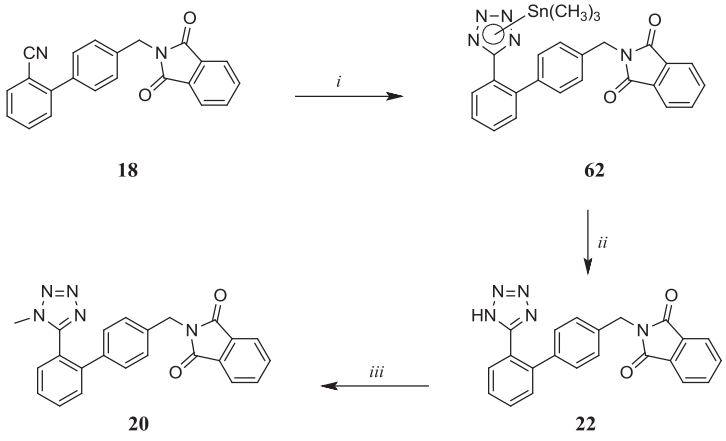

Scheme 4. Reagents and conditions: (i) $(CH_3)SnN_3$, dry toluene, 110 °C; (ii) gaseous HCl, dry toluene/THF, 0 °C; (iii) CH_3I, K_2CO_3, rt. then reflux.

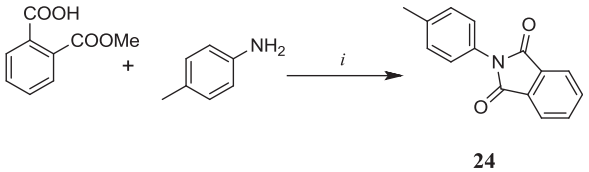

Scheme 5. Reagents and conditions: (i) EEDQ, Et_3N, $CHCl_3$, reflux.

interaction. On the other hand, the compounds of the present paper have spacers between the phthalimide core and the aromatic moiety, therefore only a folded conformation is possible for binding into *Ef*TS active site; the obtained results suggest that this decreases the inhibition activity and complex stability. The structure determination of *Ef*TS complexes with rigid inhibitors (e.g. **6A**, **8A** and **12A**) could further clarify the potential of phthalimide derivatives

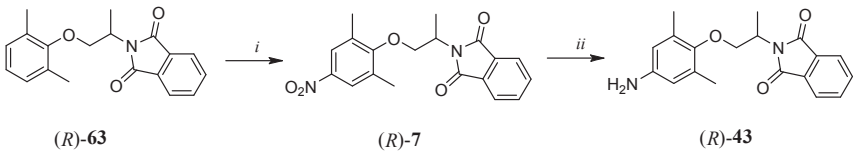

Scheme 6. Reagents and conditions: (i) $NaNO_3$, TFA, rt, (ii) 10% Pd/C, abs EtOH, rt.

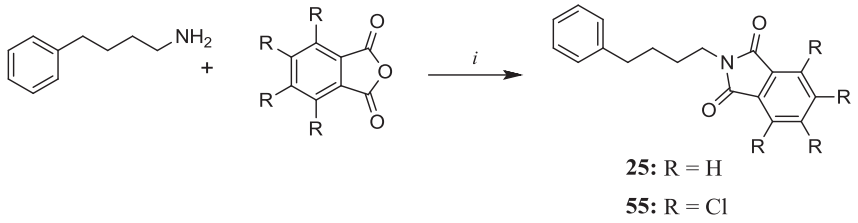

Scheme 7. Reagents and conditions: (i) Et_3N, toluene, reflux.

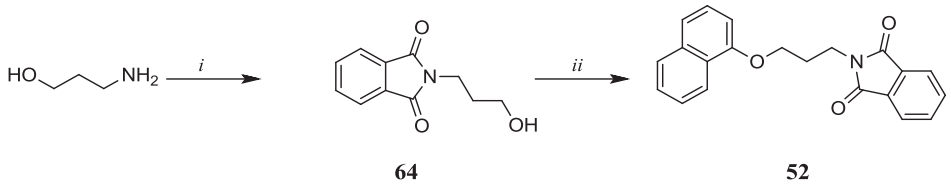

Scheme 8. Reagents and conditions: (i) phthalic anhydride, Et_3N, toluene, reflux; (ii) 1-naphthol, PPh_3, DEAD, anhyd THF, rt.

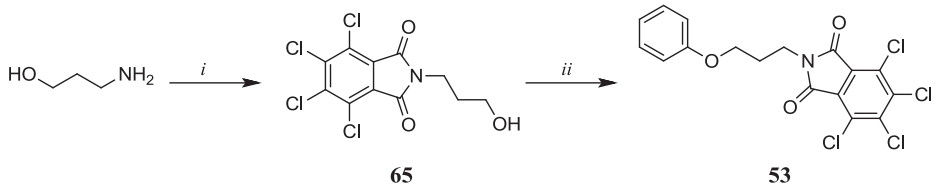

Scheme 9. Reagents and conditions: (i) tetrachlorophthalic anhydride, Et_3N, toluene, reflux; (ii) phenol, PPh_3, DEAD, anhyd THF, rt.

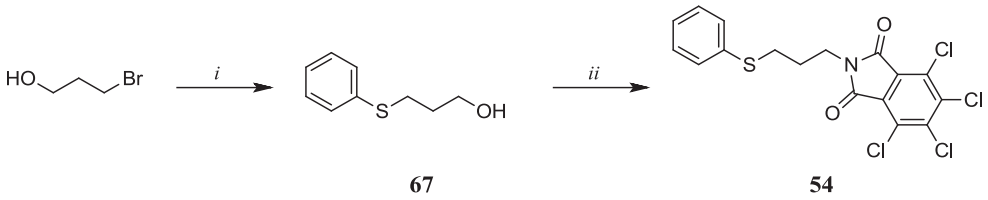

Scheme 10. Reagents and conditions: (i) thiophenol, K_2CO_3, anhyd DMF, reflux; (ii) tetrachlorophthalimide, PPh_3, DEAD, anhyd THF, rt.

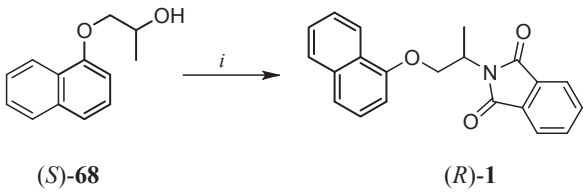

Scheme 11. Reagents and conditions: (i) phthalimide, PPh_3, DIAD, dry THF, rt.

as tool for the *Ef*TS inhibition. The structure of *Ef*TS-MTX shows the same subunit heterogeneity observed for the *Ef*TS-(*S*)-**12** complex with two subunits (A and B) in "open" conformation and two in "closed" conformation with the MTX inhibitor bound. At variance with the previous structure, no 5-HMHF is found, possibly suggesting that MTX has replaced the folate derivative in both subunits. The pose and the electron density of MTX bound to *Ef*TS is reported in Fig. 5A and compared with the *Ef*TS-(*S*)-**12** in Fig. 5B. (*S*)-**12** and MTX assume essentially the same pose in the *Ef*TS active site and make similar interactions. The glutamic acid moiety terminal portion of MTX, that is missing in (*S*)-**12**, does not interact with the cavity, the closest approach being that of the vicinal carboxylate group of MTX lying at 3.4 Å and 4.0 Å from the side chains of Phe227 and Lys48, respectively. It is noteworthy that, as for the (*S*)-**12** *Ef*TS structure, dUMP is not bound into the active site of the *Ef*TS-MTX complex and the binding site of dUMP phosphate is occupied by a sulfate anion in both crystal structures. Comparison

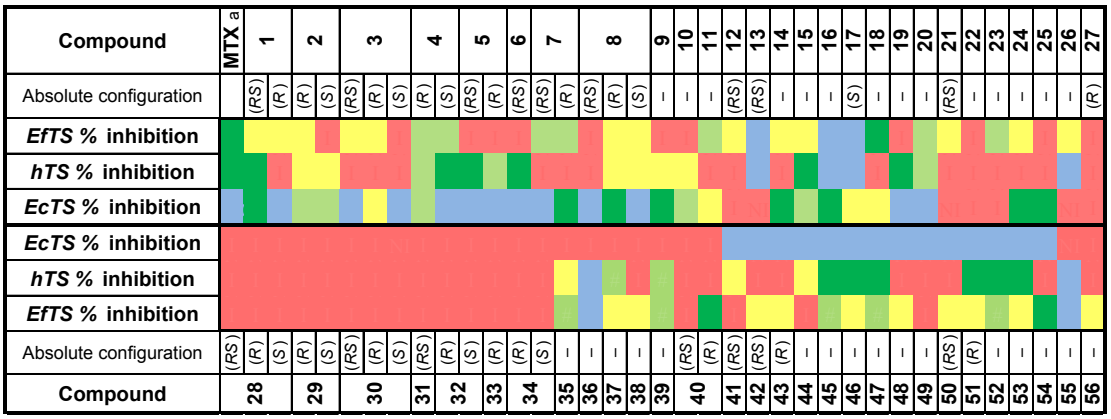

Fig. 2. Inhibitory activity of compounds 1–56 against *Ef*TS, hTS and *Ec*TS. The compound activity is given as % of inhibition at 100 μM. Color code: dark green (values between 100 and 35), light green (values between 34 and 10), yellow (values lower than 10), red (no detectable inhibition at 100 μM) and light blue (not tested). [a] MTX is the reference compound. K_i *Ef*TS = 13 μM. (For interpretation of the references to colour in this figure legend, the reader is referred to the web version of this article.)

of the *Ef*TS-(*S*)-**12** and MTX structures with the closed form of human TS with bound raltitrexed (PDB: 1HVY) suggests a possible way to increase specificity and affinity of inhibitors towards the bacterial enzyme. The only relevant difference between human TS and *Ef*TS cavity consists in the presence of Glu88 that is replaced by Ala111 in the human enzyme. The side chain of Glu88 is located at about 7.0 Å from the dimethyl benzene ring of (*S*)-**12** and from the PABA ring of MTX. The design and synthesis of (*S*)-**12** derivatives where the benzene ring bears meta substituents able to form H-bonds with the side chain of Glu88 could lead to an increased affinity towards *Ef*TS together with specificity.

3. Conclusions

Aiming to obtain novel specific inhibitors of *Ef*TS enzyme, we combined an *in vitro* target-based screening approach with X-ray crystallographic studies. The most interesting compounds (**18**, (*R*)-**40** and **54**) showed K_i of 13–25 μM, with compound (*R*)-**40** being the most potent and selective towards *Ef*TS with respect to the human enzyme. X-ray crystallographic studies were carried out on structurally different phthalimides. The X-ray crystal structure of *Ef*TS in complex with a low affinity inhibitor, (*S*)-**12**, was determined and refined. In this structure *Ef*TS behaves as half-site enzyme. According to the crystallographic structure, compound (*S*)-**12** binds into the active site with an orientation analogue to that of folate metabolites, thus suggesting a competitive behavior with respect to the folate co-substrate. One subunit binds a folate metabolite (5-HMHF), suggesting that high affinity ligands are needed to fully displace the substrates in both the subunits. We can conclude that target druggability is affected by the presence of folate analogues bound into one *Ef*TS subunit. Moreover, we solved the X-ray crystal structure of *Ef*TS in complex with MTX (K_i = 13 μM) in which the folate metabolites, such as 5-HMHF, are not bound. This confirms the ability of high affinity ligands to displace the metabolites from the binding site. The present study discloses the *Ef*TS druggability and represents an interesting starting point for a target-based drug design aimed at developing more potent *Ef*TS inhibitors and antibacterial drugs.

4. Experimental section

4.1. Chemistry

The synthesis of compounds **1,4,10,21,23** [19], **2,12,42,50** [21,22], **3,6,41** [23,24], **5,27–32,56** [25], **9,11,14–16,26,35,44–49,65** [27], **18** [29], **19** [47], **34** [30], **36–40,51** [18], **63** [31,32] has been already published in literature. For compound **7**, only the (*R*)-enantiomer, not previously reported, has been herein described, while (*RS*)-**7** is described in the literature [26]. Compounds **22, 24, 25, 52, 55** had been previously described in the literature (as referenced below) but not fully characterized and/or synthesized following different procedures. All chemicals were purchased from Sigma-Aldrich or Lancaster in the commercially available highest quality. Solvents were reagent grade unless otherwise indicated. Yields refer to purified products and were not optimized (Table S4, see Supplementary Material). The structures of the compounds were confirmed by routine spectrometric analyses. Only spectra for compounds not previously described are given. Melting points (mp) were determined on a Gallenkamp melting point apparatus in open glass capillary tubes and are uncorrected (Table S4, see Supplementary Material). The infrared spectra were recorded on a Perkin-Elmer SpectrumOne FT spectrophotometer and band positions are given in reciprocal centimetres (cm^{-1}). ^1H NMR and ^{13}C NMR spectra were recorded on a Varian VX Mercury spectrometer operating at 300 and 75 MHz for ^1H and ^{13}C, respectively, using $CDCl_3$ and DMSO-d_6 as solvents. Chemical shifts are reported in parts per million (ppm) relative to solvent resonance: $CDCl_3$, δ 7.26 (^1H NMR) and δ 77.3 (^{13}C NMR); DMSO-d_6, δ 2.48 (^1H NMR). *J* values are given in Hz (NMR Spectra for compounds 2, 3, 5, 6, 9, 11, 12, 14, 16, 18, 36–42, 44–50 are available in the Supplementary Material.). Gas chromatography (GC)/mass spectroscopy (MS) was performed on a Hewlett-Packard 6890–5973 MSD at low resolution. Liquid chromatography (LC)/mass spectroscopy (MS) was performed on a spectrometer Agilent 1100 series LC-MSD Trap System VL. The molecular ion was designed as "M^+". Elemental analyses were performed on a Eurovector Euro EA 3000 analyzer and the data for C, H, N were within ±0.4 of theoretical values (Table S3, see Supplementary Material). Optical rotations were measured on a Perkin Elmer (Norwalk, CT) Mod 341 spectropolarimeter; concentrations are expressed in g/100 mL, and the cell length was 1 dm, thus $[\alpha]_D^{21}$ values are given in units of 10^{-1} deg cm^2 g^{-1}. Chromatographic separations were performed on silica gel columns by flash chromatography (Kieselgel 60, 0.040–0.063 mm, Merck, Darmstadt, Germany) as previously described [48,49].

4.1.1. (*R*)-2-[1-Methyl-2-(1-naphthyloxy)ethyl]-1H-isoindole-1,3(2H)-dione (*R*)-**1**

Prepared as reported below for (*RS*)-**8** starting from (*S*)-**68** and

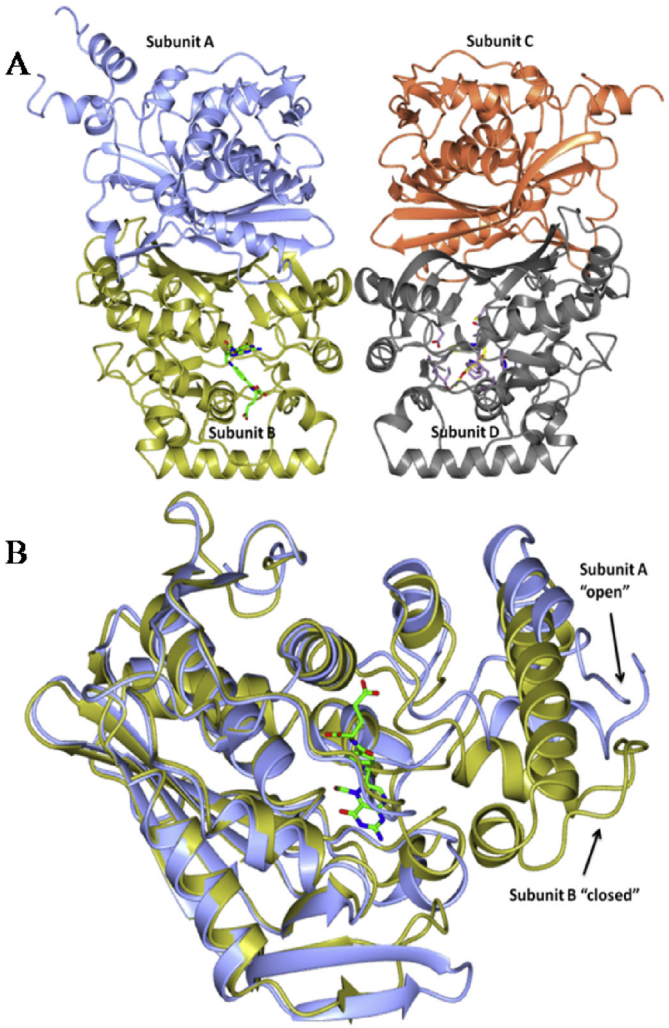

Fig. 3. *Ef*TS x-ray crystallographic structure. (A) The *Ef*TS crystal asymmetric unit content. The two subunits of each heterodimer differ in the conformation of the small domain due to the presence of a ligand bound to the active site cavities. The subunit having a ligand bound are in closed conformation, while the unbound subunits are in open conformation. (B) comparison of closed and open conformations by superimposing subunit A (open; light blue ribbon) and B (closed; gold ribbon) of 4O7U. The 5-HMHF molecule is represented to show the position of the active site cavity. (For interpretation of the references to colour in this figure legend, the reader is referred to the web version of this article.)

phthalimide. Yield: 57%; mp 79–81 °C (EtOAc/hexane); $[\alpha]_D^{20} = -38$ (*c* 1, $CHCl_3$). Spectroscopic and spectrometric data were in agreement with those found in the literature for the racemate [19]. Anal. Calcd. for $C_{21}H_{17}NO_3$%: C, 76.12; H 5.17; N 4.23. Found: C, 75.85; H 5.16; N 4.31.

*4.1.1.1. (R)-2-[2-(2,6-Dimethyl-4-nitrophenoxy)-1-methylethyl]-1H-isoindole-1,3(2H)-dione (R)-**7**.* 0.65 g (2.1 mmol) of (*R*)-**63** were dissolved in 5 mL of trifluoroacetic acid at room temperature. Then, 0.22 g (2.5 mmol) of sodium nitrate were added to the solution in small portions during the period of 60 min. The mixture was stirred overnight, then diluted with 15 mL of diethyl ether and 3 mL of brine. The aqueous phase was extracted with Et_2O for three times. The organic layers, washed with 20% NaOH aqueous solution, were dried over anhydrous Na_2SO_4 to give 0.65 g (85%) of an orange foam which was recrystallized from Et_2O/petroleum ether to give orange crystals: mp 105–106 °C (Et_2O/petroleum ether); $[\alpha]_D^{20} = -30$ (*c* 2, $CHCl_3$); ^{1}H NMR ($CDCl_3$): δ 1.55 (d, J = 7.2 Hz, 3H, C*H*$_3$CH), 2.26 (s, 6H, C*H*$_3$), 3.96 (dd, J = 9.3, 5.5 Hz, C*H*HCH), 4.48 (t, J = 9.3 Hz, 1H, CH*H*CH), 4.80–4.95 (m, 1H, C*H*), 7.70–7.76 (m, 2H, Ar*H*C-5,6), 7.82–8.00 (m, 4H, ArO*H*C-3,5, Ar*H*C-4,7). Other spectroscopic data were in agreement with those reported in the literature for the racemate [26]. Anal. calcd for $C_{19}H_{18}N_2O_5$%: C, 64.40; H 5.12; N 7.91. Found: C, 64.45; H 5.16; N 7.95.

*4.1.1.2. (RS)-2-[2-(2,6-dimethylphenoxy)propyl]-1H-isoindole-1,3(2H)-dione (RS)-**8**.* To a stirred solution of (*RS*)-**61** (1.97 g, 10.9 mmol), phthalimide (2.40 g, 16.3 mmol) and triphenylphosphine (4.28 g, 16.3 mmol) in dry THF (100 mL), under N_2 atmosphere, a solution of diisopropylazodicarboxylate (DIAD) (3.30 g, 16.3 mmol) in dry THF (50 mL) was added dropwise. The mixture was stirred at room temperature for 24 h. The solvent was then evaporated under reduced pressure, Et_2O was added and the precipitate formed was filtered off. The filtrate was evaporated in vacuum and the residue was purified by flash chromatography (eluent EtOAc/petroleum ether 2:8) to give 3.24 g of a white solid (96%) which was recrystallized from EtOAc: mp 90–91 °C; IR (KBr): 1772, 1717 (C=O) cm^{-1}; ^{1}H NMR ($CDCl_3$): δ 1.19 (d, J = 6.0 Hz, 3H, C*H*$_3$CH), 2.22 (s, 6H, C*H*$_3$Ar), 3.85 (dd, J = 13.5, 6.3 Hz, 1H, C*H*H), 4.07 (dd, J = 13.6, 7.0 Hz, 1H, CH*H*), 4.52 (sextet, J = 6.3 Hz, 1H, C*H*), 6.82–7.0 (m, 3H, Ar), 7.68–7.78 (m, 2H, Ar), 7.82–7.90 (m, 2H, Ar); ^{13}C NMR ($CDCl_3$):δ 17.3 (2C), 18.2 (1C), 43.4 (1C), 74.2 (1C), 123.5 (2C), 123.7 (1C), 129.2 (2C), 131.4 (2C), 132.2 (2C), 134.2 (2C), 153.1 (1C), 168.5 (2C); GC/MS (70 eV) *m/z* (%) 309 (M^+, 16), 188 (100). Anal. calcd for $C_{19}H_{19}NO_3.0.25H_2O$ %: C, 72.71; H 6.26; N 4.46. Found: C, 72.85; H 6.19; N 4.51.

*4.1.1.3. (R)-2-[2-(2,6-Dimethylphenoxy)propyl]-1H-isoindole-1,3(2H)-dione (R)-**8**.* Prepared as reported above for (*RS*)-**8** starting from (*R*)-**61**. Yield: 87%; white crystals: mp 69–70 °C (EtOAc); $[\alpha]_D^{20} = -81$ (*c* 2, $CHCl_3$). Spectroscopic data were in agreement with the racemate. Anal. calcd for $C_{19}H_{19}NO_3$%: C, 73.77; H 6.19; N 4.53. Found: C, 73.82; H 6.24; N 4.57.

*4.1.1.4. (S)-2-[2-(2,6-Dimethylphenoxy)propyl]-1H-isoindole-1,3(2H)-dione (S)-**8**.* Prepared as reported above for (*RS*)-**8** starting from (*S*)-**61**. Yield: 80%; white crystals: mp 70–71 °C (EtOAc); $[\alpha]_D^{20} = +79$ (*c* 2, $CHCl_3$). Spectroscopic data were in agreement with the racemate. calcd for $C_{19}H_{19}NO_3$%: C, 73.77; H 6.19; N 4.53. Found: C, 73.59; H 6.18; N 4.57.

*4.1.1.5. 2-[1-(4-Hydroxy-2,6-dimethylphenoxy)propan-2-yl]-1H-isoindole-1,3(2H)-dione (RS)-**13**.* A solution of (*RS*)-**12** (0.82 g, 2.23 mmol) in THF (6 mL) and 10% HCl solution (5 mL) was stirred in an ice-bath for 3 h. Then the mixture was stirred at room temperature for 48 h. The solvent was evaporated under vacuum and extracted with EtOAc. The organic layer was dried (Na_2SO_4) to give a slightly yellowish solid which was recrystallized from EtOAc/petroleum ether to give 0.43 g (59%) of slightly yellowish crystals: mp 178–179 °C; IR (KBr): 3412 (OH), 1770, 1699 (C=O); ^{1}H NMR ($CDCl_3$): δ 1.53 (d, J = 6.9 Hz, 3H, C*H*$_3$CH), 2.12 (s, 6H, C*H*$_3$Ar), 3.84 (dd, J = 9.2, 5.6 Hz, 1H, C*H*HCH), 4.29 (t, J = 9.2 Hz, 1H, CH*H*CH), 4.58 (br s, 1H, O*H*), 4.76–4.92 (m, 1H, C*H*), 6.41 (s, 2H, Ar), 7.65–7.74 (m, 2H, Ar), 7.78–7.90 (m, 2H, Ar); ^{13}C NMR ($CDCl_3$): δ15.4 (1C), 16.5 (2C), 47.4 (1C), 72.2 (1C), 115.2 (2C), 123.4 (2C), 132.1 (2C), 132.2 (2C), 134.2 (2C), 149.3 (1C), 151.5 (1C), 168.7 (2C); GC/MS (70 eV) *m/z* (%) 325 (M^+, 5), 188 (100). Anal. calcd for $C_{19}H_{19}NO_4.0.20H_2O$ %: C, 69.37; H 5.94; N 4.26. Found: C, 69.59; H 5.84; N 4.37.

*4.1.1.6. (S)-**2**-(2-Iodo-1-phenylethyl)-1H-isoindole-1,3(2H)-dione (S)-**17**.* Into a stirred ice-cooled solution of (*S*)-**33** (1.74 g, 6.5 mmol) in dry toluene (30 mL) under N_2 atmosphere, HI was bubbled until saturation occurred. The mixture was stirred at −5 °C for 1 h and at

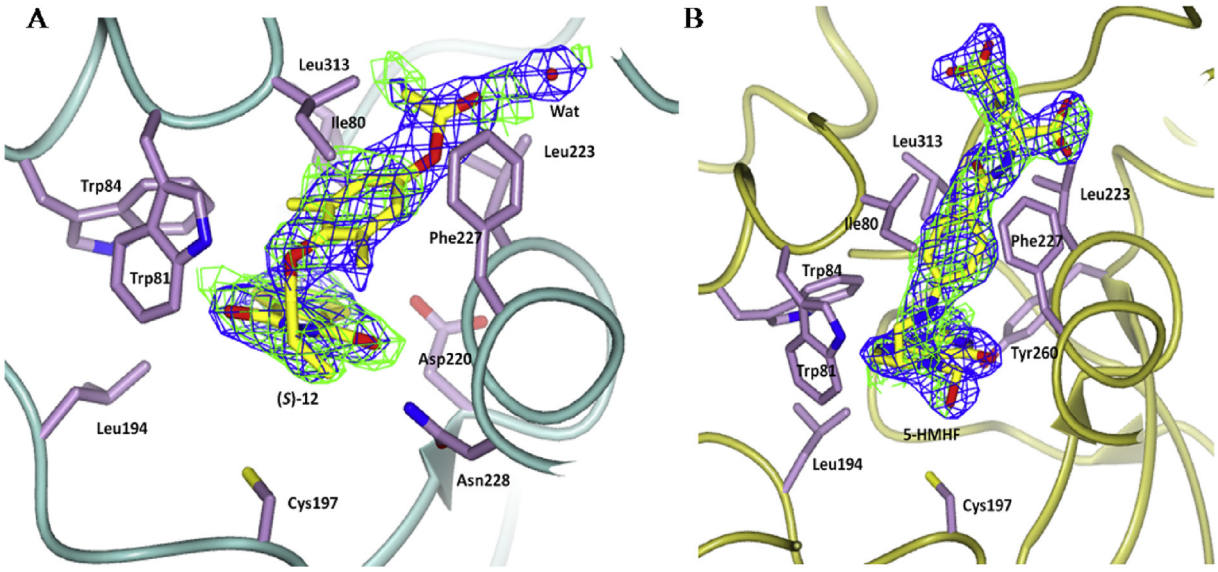

Fig. 4. Detailed view of the binding ligands. (A) Stick representation of the (*S*)-**12** inhibitor (yellow) bound to *Ef*TS with superimposed the 2Fo-Fc electron density map at 1.3 σ (blue wire), computed with refined phases and the omit map (green wire) contoured at 3.0 σ. Cys197 is also shown as sticks together with other relevant residues in the active site cavity. (B) Stick representation of 5-HMHF (yellow) bound to *Ef*TS with superimposed the 2Fo-Fc electron density map at 1.3 σ (blue wire), computed with refined phases and the omit map (green wire) contoured at 3.0 σ. Cys197 is also shown as sticks together with other relevant residues in the active site cavity. Notice the different extent of the omit map in the PABA moiety of 5-HMHF with respect to the same region in Fig. 4A. (For interpretation of the references to colour in this figure legend, the reader is referred to the web version of this article.)

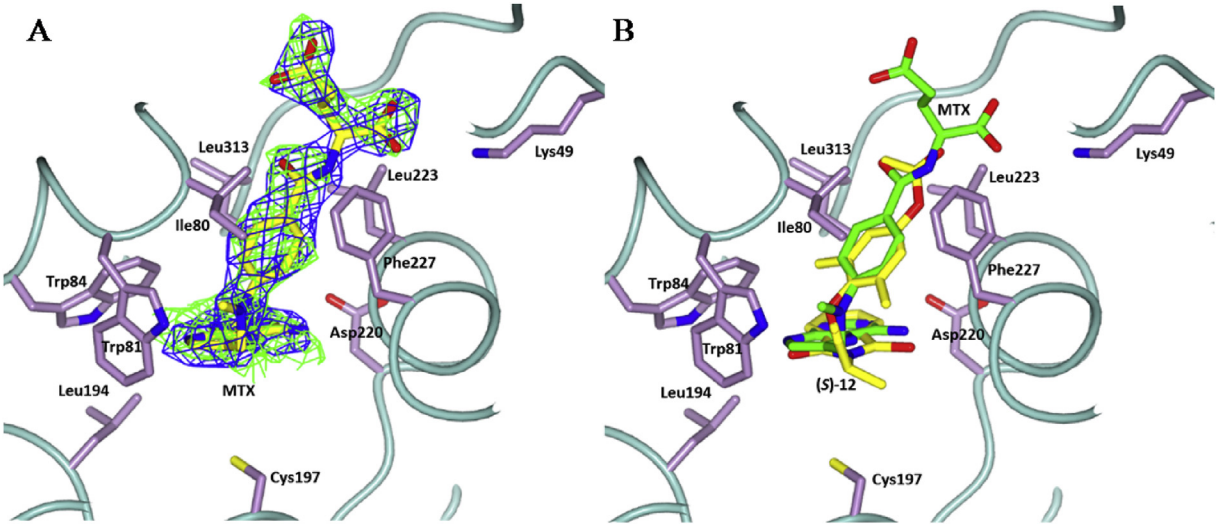

Fig. 5. The binding of MTX to *Ef*TS. (A) Stick representation of the MTX inhibitor (yellow) bound to *Ef*TS with superimposed the 2Fo-Fc electron density map at 1.3 σ (blue wire), computed with refined phases and the omit map (green wire) contoured at 3.0 σ. Cys197 is also shown as sticks together with other relevant residues in the active site cavity. (B) Least-squares superimposition of MTX (green sticks) and (*S*)-**12** (yellow sticks) bound to *Ef*TS. Notice the similarity of the pose. (For interpretation of the references to colour in this figure legend, the reader is referred to the web version of this article.)

room temperature for 48 h. The solvent was then evaporated under vacuum and the residue, taken up with EtOAc, was washed with 6 N NaOH, 2 N HCl, and brine. The organic layer was dried (Na_2SO_4) and concentrated under vacuum to give 1.7 g (70%) of a slightly yellowish solid which was recrystallized from MeOH to give (*S*)-**17** as white crystals: mp 123–124 °C; $[\alpha]_D^{20} = -16$ (*c* 2, $CHCl_3$); IR (KBr): 1780, 1707 (C=O); ^{1}H NMR ($CDCl_3$): δ 3.83 (dd, 1H, *J* = 10.5, 5.2 Hz, C*H*H), 4.53 (t, 1H, *J* = 10.8 Hz,C*H*), 5.56 (q, 1H, *J* = 5.2 Hz, CH*H*), 7.28–7.38 (m, 3H, Ar), 7.50–7.58 (m, 2H, Ar), 7.68–7.76 (m, 2H, Ar), 7.82–7.88 (m, 2H, Ar); ^{13}C NMR ($CDCl_3$): δ 4.8 (1C), 57.8 (1C), 123.8 (2C), 128.1 (2C), 128.9 (2C), 129.2 (1C), 131.8 (2C), 134.5 (1C), 138.1 (2C), 168.1 (2C); GC/MS (70 eV) *m/z* (%) 377 (M^+, <1), 250 (100). Anal. calcd for $C_{16}H_{12}NO_2I$ %: C, 50.95; H 3.21; N 3.71. Found: C, 51.15; H 3.25; N 3.79.

4.1.1.7. 2-{[2′-(1-Methyl-1H-tetrazol-5-yl)biphenyl-4-yl]methyl}-1H-isoindole-1,3(2H)-dione ***20***. Potassium carbonate (65.2 g, 0.47 mmol) was added to a solution of **22** (0.15 g, 0.39 mmol) in 10 mL of acetone. The mixture was stirred at room temperature for 30 min, and then methyl iodide (0.11 g, 0.77 mmol) was added. The reaction mixture was refluxed for 2 h. After cooling, the reaction mixture was filtered and evaporated. The residue was extracted with EtOAc and washed twice with H_2O. After drying (Na_2SO_4), the organic phase was evaporated to afford a crude solid which was

purified by crystallization from $CHCl_3$/hexane affording 83 mg (54%) of white crystals: mp 210–211 °C; IR (KBr): 1766, 1705 (C=O); ^{1}H NMR ($CDCl_3$):δ 4.22 (s, 3H, CH_3), 4.82 (s, 2H, CH_2), 7.04–7.16 (m, 2H, Ar), 7.28–7.38 (m, 2H, Ar), 7.40–7.90 (m, 8H, Ar); ^{13}C NMR ($CDCl_3$): δ 33.8 (1C), 41.3 (2C), 122.6 (1C), 123.6 (2C), 123.7 (1C), 128.2 (1C), 128.4 (2C), 129.1 (1C), 130.6 (2C), 131.7 (1C), 132.0 (1C), 134.3 (2C), 135.3 (1C), 136.6 (1C), 138.7 (1C), 141.5 (1C), 168.3 (2C); GC/MS (70 eV) *m/z* (%) 395 (M^+, 34), 394 (100). Anal. calcd for $C_{23}H_{17}N_5O_2$%: C, 69.86; H 4.33; N 17.71. Found: C, 69.47; H 4.37; N 17.43.

4.1.1.8. 2-{[2′-(1H-tetrazol-5-yl)biphenyl-4-yl]methyl}-1H-isoindole-1,3(2H)-dione ***22***. A suspension of compound **62** (0.60 g, 1.1 mmol) in a mixture of toluene (8 mL) and THF (2 mL) was stirred in an ice bath. Gaseous HCl was then added to give a clear solution followed by precipitation of the desired product. The precipitate was filtered, and the filtrate was washed with toluene to give a white solid (0.40 g, 96%): mp: >250 °C; IR (KBr): 3458 (NH), 1767, 1714 (C=O), 1463, 1252 (*N*–N=N) cm^{-1}; ^{1}H NMR (DMSO-d_6): δ 4.72 (s, 2H, CH_2), 7.04 (d, J = 8.2 Hz, 2H, Ar), 7.23 (d, J = 8.2 Hz, 2H, Ar), 7.46–7.70 (m, 4H, Ar), 7.78–7.96 (m, 4H, Ar), 16.4 (1H, N*H*); LC/MS *m/z* 380 [M^+ – 1]. Other spectroscopic data were in agreement with the literature [50]. Anal. calcd for $C_{22}H_{15}N_5O_2.0.50H_2O$ %: C, 67.68; H 4.13; N 17.94. Found: C, 67.73; H 4.03; N 17.70.

4.1.1.9. 2-(4-Methylphenyl)-1H-isoindole-1,3(2H)-dione ***24***. EEDQ (1.48 g, 6 mmol), *p*-toluidine (0.59 g, 5.5 mmol) and Et_3N (1.04 mL, 7.5 mmol) were successively added to a stirring solution of 2-(methoxycarbonyl)benzoic acid (1.0 g, 5 mmol) in $CHCl_3$ (160 mL). The reaction mixture was heated under reflux for 6 h. The solvent was removed under reduced pressure and the residue, taken up with EtOAc, was washed three times with 2 N HCl, twice with 2 N NaOH, and then dried over anhydrous Na_2SO_4. The organic phase was evaporated to afford a crude solid which was purified by crystallization from $CHCl_3$/hexane to give 0.90 g (67%) of **24** as beige crystals: mp 205–206 °C; IR (KBr): 1747, 1716 (C=O); ^{1}H NMR ($CDCl_3$):δ 2.41 (s, 3H, CH_3), 7.31 (s, 4H, Ar), 7.74–7.82 (m, 2H, Ar), 7.92–7.99 (m, 2H, Ar); GC/MS (70 eV) *m/z* (%) 237 (M^+, 100). Other spectroscopic data were in agreement with the literature [51]. Anal. calcd. for $C_{15}H_{11}NO_2.0.20H_2O$ %: C, 74.80; H 4.77; N 5.82. Found: C, 75.06; H 5.08; N 6.00.

4.1.1.10. 2-(4-Phenylbutyl)-1H-isoindole-1,3(2H)-dione ***25***. Prepared as reported for compound **55** starting from 4-phenylbutan-1-amine and phthalic anhydride. Yield: 62%; white solid: mp 84–85 °C. Spectroscopic data were in agreement with the literature [52].

*4.1.1.11. (R)-2-(2-Hydroxy-1-phenylethyl)-1H-isoindole-1,3(2H)-dione (R)-****33***. Prepared as reported above for compound **64** starting from (*R*)-phenylglycinol and phthalic anhydride. Yield: 88%; white crystals: $[\alpha]_D^{20}$ = + 41 (*c* 2, $CHCl_3$); IR (neat): 3464 (OH), 1772, 1710 (C=O); ^{1}H NMR ($CDCl_3$): δ 2.64 (br s, 1H, O*H*), 4.21 (dd, J = 11.6, 5.0 Hz, 1H, C*H*H), 4.65 (dd, J = 11.6, 9.3 Hz, 1H, CH*H*), 5.41–5.53 (m, 1H, C*H*), 7.23–7.38 (m, 3H, Ar), 7.40–7.50 (m, 2H, Ar), 7.63–7.73 (m, 2H, Ar), 7.74–7.85 (m, 2H, Ar). Other spectroscopic data were in agreement with those reported in the literature [53,54]. Anal. calcd. for $C_{16}H_{13}NO_3$%: C, 71.90; H 4.90; N 5.24. Found: C, 72.24; H 4.99; N 5.40.

*4.1.1.12. (S)-2-(2-Hydroxy-1-phenylethyl)-1H-isoindole-1,3(2H)-dione (S)-****33***. Prepared as reported above for compound **64** starting from (*S*)-phenylglycinol and phthalic anhydride. Yield: 85%; slightly yellowish crystals: $[\alpha]_D^{20}$ = –32 (*c* 2, $CHCl_3$). Other spectroscopic data were in agreement with those reported in the literature for the *R*-enantiomer [53,54].

*4.1.1.13. (R)-2-[1-(4-amino-2,6-dimethylphenoxy)propan-2-yl]-1H-isoindole-1,3(2H)-dione hydrochloride (R)-****43***. Catalytic hydrogenation of (*R*)-**7** (0.35 g, 1.0 mmol) in 10 mL of absolute EtOH was conducted at room temperature for 12 h in the presence of 10% palladium on carbon at 10 bar. The catalyst was filtered off and the solvent was removed under reduced pressure to give 0.23 g (70%) of the free amine (*R*)-**43** as a yellow oil which was converted into its hydrochloride salt by dissolving the free base in a small amount of aqueous 1 N HCl and azeotropically removing water. The crude solid obtained was recrystallized from EtOH/Et_2O: mp 256–258 °C; $[\alpha]_D^{20}$ = –42 (*c* 2, MeOH). Spectroscopic and spectrometric data were in agreement with those found in the literature for the racemate [26]. Anal. calcd for $C_{19}H_{20}N_2O_3$.HCl.0.33H_2O %: C, 62.21; H 5.95; N 7.64. Found: C, 62.16; H 6.06; N 7.24.

4.1.1.14. 2-[3-(Naphthalen-1-yloxy)propyl]-1H-isoindole-1,3(2H)-dione ***52***. Prepared as reported above for (*RS*)-**8** starting from (*R*)-**64** and 1-naphthol using diethyl azodicarboxylate (DEAD) instead of DIAD. Yield: 36%; mp 150–151 °C (EtOAc/hexane), lit [55] 154–154.5 °C; IR (KBr): 1765, 1713 (C=O) cm^{-1}; ^{1}H NMR ($CDCl_3$): δ 2.34(quintet, J = 6.9 Hz, 2H, $CH_2CH_2CH_2$),4.01 (t, J = 6.8 Hz, 2H, CH_2N),4.22 (t, J = 6.0 Hz, 2H, CH_2O), 6.76 (d, J = 6.6 Hz, 1H, Ar), 7.33–7.44 (m, 4H, Ar), 7.64–7.68 (m, 2H, Ar),7.75 (d, J = 8.2 Hz, 1H, ArO), 7.78–7.82 (m, 2H, Ar),8.16 (d, J = 7.7, 1H, Ar); ^{13}C NMR ($CDCl_3$): δ 28.7 (1C), 35.9 (1C), 66.1 (1C), 104.7 (1C), 120.6 (1C), 122.1 (1C), 123.4 (2C), 125.3 (1C),125.7 (1C), 126.0 (1C), 126.5 (1C), 127.6 (1C), 132.4 (2C), 134.1 (2C), 134.6 (1C), 154.6 (1C), 168.6 (2C); GC/MS(70 eV) *m/z* (%) 331 (M^+, 13), 188 (100).

4.1.1.15. 4,5,6,7-Tetrachloro-2-(3-phenoxypropyl)-1H-isoindole-1,3(2H)-dione ***53***. Prepared as reported above for (*RS*)-**8** starting from **65** and phenol using diethyl azodicarboxylate (DEAD) instead of DIAD. Yield: 30%; mp 211–212 °C (EtOAc/hexane); IR (KBr): 1777, 1712 (C=O) cm^{-1}; GC/MS (70 eV) *m/z* (%) 419 (M^+, 6), 326 (100). Anal. calcd for $C_{17}H_{11}Cl_4NO_3.0.50H_2O$ %: C, 47.70; H 2.83; N 3.27. Found: C, 47.62; H 2.65; N 3.41.

4.1.1.16. 4,5,6,7-Tetrachloro-2-[3-(phenylsulfanyl)propyl]-1H-isoindole-1,3(2H)-dione ***54***. Prepared as reported above for (*RS*)-**8** starting from **67** and tetrachlorophthalimide, using diethylazodicarboxylate (DEAD) instead of DIAD. Yield: 20%; mp 140–141 °C (THF/petroleum ether); IR (KBr): 1775, 1713 (C=O) cm^{-1}; ^{1}H NMR ($CDCl_3$): δ 1.97–2.04 (m, 2H, $CH_2CH_2CH_2$), 2.93 (t, J = 7.1 Hz, 2H, CH_2S), 3.83 (t, J = 7.0 Hz, 2H, CH_2N), 7.15–7.35 (m, 5H, Ar); ^{13}C NMR ($CDCl_3$): δ 27.9 (1C), 31.7 (1C),38.1 (1C),126.7 (2C),127.8 (1C), 129.2 (2C), 129.8 (2C), 130.3 (2C), 135.7 (2C),140.3 (1C), 163.7 (2C); GC/MS (70 eV) *m/z* (%) 433 (M^+, 54), 149 (100).

4.1.1.17. 4,5,6,7-Tetrachloro-2-(4-phenylbutyl)-1H-isoindole-1,3(2H)-dione ***55***. A mixture of 4-phenylbutan-1-amine (2.0 g, 13.4 mmol), tetrachlorophthalic anhydride (3.83 g, 13.4 mmol), triethylamine (0.13 g, 1.34 mmol) in toluene (20 mL) was heated under reflux in a flask fitted with a Dean–Stark tube for 7 h. During this period, the temperature of the oil bath is maintained at about 130 °C and water separates. All volatile matter were then evaporated under vacuum and the solid residue was taken up with EtOAc and washed with 2 N HCl, $NaHCO_3$, and H_2O. The organic phase was dried (Na_2SO_4) and concentrated under vacuum to give a white solid which was recrystallized from EtOAc/hexane to give 3.90 g (70%) of white crystals: mp 119–120 °C. Other spectroscopic data were in agreement with the literature [52]. Anal. calcd for $C_{18}H_{13}Cl_4NO_2$%: C, 51.83; H 3.14; N 3.36. Found: C, 51.71; H 3.13; N 3.44.

*4.1.1.18. (RS)-Ethyl 2-(2,6-dimethylphenoxy)propanoate (RS)-**59**.* Sodium (0.38 g, 16.5 mmol) was added in small pieces to absolute EtOH (30 mL) and the mixture was heated at 70 °C. After completion of sodium dissolution, a solution of 2,6-dimethylphenol (2.0 g, 16.5 mmol) in absolute EtOH (15 mL) was added dropwise. After 30 min, a solution of (*RS*)-ethyl 2-bromopropanoate [(*RS*)-**57**] (2.98 g, 16.5 mmol) in absolute EtOH (15 mL) was added dropwise and the mixture was heated at reflux for 5 h. The solid residue was filtered off, the solvent was evaporated in vacuum and the residue was taken up with diethyl ether, washed with 2 N NaOH and dried (Na_2SO_4). Removal of the solvent under vacuum gave 3.11 g (85%) of (*RS*)-**59** as a yellow oil: IR (neat): 1737 (C=O) cm^{-1}; ^1H NMR ($CDCl_3$): δ 1.28 (t, 3H, J = 7.1 Hz, CH_3CH_2), 1.53 (d, 3H, J = 6.6 Hz, CH_3CH), 2.28 (s, 6H, CH_3Ar), 4.23 (q, 2H, J = 7.1 Hz, CH_2), 4.49 (q, 1H, J = 6.6 Hz, C*H*), 6.86–6.94 (m, 1H, Ar), 6.95–7.03 (m, 2H, Ar); ^{13}C NMR ($CDCl_3$): δ 14.4 (1C), 17.2 (2C), 18.7 (1C), 61.3 (1C), 77.1 (1C), 124.2 (1C), 129.3 (2C), 131.1 (2C), 154.8 (1C), 172.3 (1C); GC/MS (70 eV) *m/z* (%) 222 (M^+, 91), 149 (100).

*4.1.1.19. (R)-Methyl 2-(2,6-dimethylphenoxy)propanoate (R)-**60**.* Prepared as reported above for (*RS*)-**8** starting from 2,6-dimethylphenol and ethyl (*S*)-(−)-lactate [(*S*)-**58**]. Yield: 72%; slightly yellowish oil:$[\alpha]_D^{20} = +40$ (*c* 2.1, $CHCl_3$). Spectroscopic data were in agreement with the (*S*)-isomer.

*4.1.1.20. (S)-Methyl 2-(2,6-dimethylphenoxy)propanoate (S)-**60**.* Prepared as reported above for (*RS*)-**8** starting from 2,6-dimethylphenol and methyl (*R*)-(+)-lactate [(*R*)-**58**]. Yield: 37%; slightly yellowish oil: $[\alpha]_D^{20} = -39$ (*c* 2.1, $CHCl_3$); IR (neat): 1759 (C=O) cm^{-1}; ^1H NMR ($CDCl_3$):δ 1.53 (d, J = 6.9 Hz, 3H, CH_3CH), 2.27 (s, 6H, CH_3Ar), 3.78 (s, 3H, CH_3O), 4.51 (q, J = 6.9 Hz, 1H, C*H*), 6.88–7.04 (m, 3H, Ar); ^{13}C NMR ($CDCl_3$): δ 17.2 (2C), 18.7 (1C), 52.3 (1C), 77.0 (1C), 124.2 (1C), 129.3 (2C), 131.1 (2C), 154.7 (1C), 172.7 (1C); GC-MS (70 eV) *m/z* (%) 208 (M^+, 1), 122 (100).

*4.1.1.21. (RS)-2-(2,6-dimethylphenoxy)propan-1-ol (RS)-**61**.* To a suspension of $LiAlH_4$ (1.28 g, 33.7 mmol) in dry THF (60 mL), a solution of (*RS*)-**59** (3.74 g, 16.9 mmol) in dry THF (60 mL) under N_2 atmosphere was added. The mixture was stirred under moderate reflux for 1 h and then at room temperature for 24 h. The reaction was quenched by the careful addition of cold water until the end of gas evolution. The residue was removed by filtration and the filtrate shaken with H_2O. The aqueous phase was extracted several times with Et_2O. The combined extracts were dried over Na_2SO_4 and the filtrate was concentrated under vacuum. Purification by flash chromatography (EtOAc/petroleum ether 1:9) gave 1.85 g (61%) of (*RS*)-**61** as a colorless oil: IR (neat): 3416 (OH) cm^{-1}; ^1H NMR ($CDCl_3$): δ 1.17 (d, J = 6.3 Hz, 3H, CH_3CH), 2.28 (s, 7H, CH_3Ar + O*H*), 3.68–3.84 (m, 2H, CH_2), 4.18–4.30 (m, 1H, C*H*), 6.87–6.95 (m, 1H, Ar), 7.01 (d, J = 3.8 Hz, 2H, Ar); ^{13}C NMR ($CDCl_3$):δ 16.4 (1C), 17.4 (2C), 67.1 (1C), 78.1 (1C), 123.8 (1C), 129.3 (2C), 131.4 (2C), 154.0 (1C); GC/MS (70 eV) *m/z* (%) 180 (M^+, 37), 122 (100).

*4.1.1.22. (S)-2-(2,6-Dimethylphenoxy)propan-1-ol (S)-**61**.* Prepared as reported above for (*RS*)-**61** starting from (*S*)-**60**. Yield: 66%; colorless oil: $[\alpha]_D^{20} = +9.0$ (*c* 2.1, $CHCl_3$); IR (neat): 3401 (OH) cm^{-1};^1H NMR ($CDCl_3$): δ 1.17 (d, J = 6.3 Hz, 3H, CH_3CH), 2.21 (br s overlapping s at 2.28 ppm, exch. D_2O, 1H, O*H*), 2.28 (s overlapping br s at 2.21 ppm, 6H, CH_3Ar), 3.68–3.84 (m, 2H, CH_2), 4.18–4.29 (m, 1H, C*H*), 6.88–6.96 (m, 1H, Ar), 6.97–7.05 (m, 2H, Ar); ^{13}C NMR ($CDCl_3$):δ 16.4 (2C), 17.4 (1C), 67.1 (1C), 78.0 (1C), 123.8 (1C), 129.3 (2C), 131.4 (2C), 154.0 (1C); GC/MS (70 eV) *m/z* (%) 180 (M^+, 26), 122 (100).

*4.1.1.23. (R)-2-(2,6-Dimethylphenoxy)propan-1-ol (R)-**61**.* Prepared as reported above for (*RS*)-**61** starting from (*R*)-**60**. Yield: 62%; colorless oil: $[\alpha]_D^{20} = -9.1$ (*c* 2.1, $CHCl_3$). Spectroscopic data were in agreement with the (*S*)-isomer.

*4.1.1.24. 2-{[2'-[1-(trimethylstannyl)-1H-tetrazol-5-yl]biphenyl-4-yl} methyl]-1H-isoindole-1,3(2H)-dione **62**.* A solution of compound **18** (1.50 g, 4.44 mmol) in dry toluene (75 mL) and azidotrimethyltin (1.0 g, 4.89 mmol) was kept at 110 °C under nitrogen atmosphere for 24 h. The precipitate was filtered off and washed with hot toluene to give compound **62** as a white solid (0.90 mg, 37%): mp > 250 °C; IR (KBr): 1763, 1709 (C=O), 550 (Sn–N) cm^{-1};^1H NMR (DMSO-d_6): δ 0.32 (br s, 9H, $(CH_3)_3Sn$), 4.71 (s, 2H, CH_2), 6.98 (d, J = 8.2 Hz, 2H, Ar), 7.16 (d, J = 9.3 Hz, 2H, Ar), 7.35–7.55 (m, 4H, Ar), 7.75–7.95 (m, 4H, Ar); LC-MS *m/z* (%) 568 [M^+ + 23].

*4.1.1.25. 4,5,6,7-Tetrachloro-2-(3-hydroxypropyl)-1H-isoindole-1,3(2H)-dione **65**.* Prepared as reported above for (*R*)-**33**, starting from 3-aminopropanol and tetrachlorophthalic anhydride. Yield:32%; mp193–194 °C (EtOAc/hexane); IR (KBr): 3319 (OH), 1774, 1707 (C=O) cm^{-1}; ^1H NMR ($CDCl_3$): δ 1.85–1.92 (m, 2H, $CH_2CH_2CH_2$), 1.98 (br s, 1H, O*H*),3.64 (t, J = 5.8 Hz, 2H, CH_2N), 3.86 (t, J = 6.3 Hz, 2H, CH_2O); ^{13}C NMR ($CDCl_3$): δ 31.1 (1C), 35.7 (1C), 59.5 (1C),127.7 (2C), 129.9 (2C),140.4 (2C); 164.2 (2C); GC/MS(70 eV) *m/z* (%) 343 (M^+, 24), 298 (100). Anal. calcd for $C_{11}H_{17}Cl_4NO_3.H_2O$ %: C, 36.60; H 2.51; N 3.88. Found: C, 36.53; H 2.11; N 3.86.

*4.1.1.26. 3-(Phenylsulfanyl)propan-1-ol **67**.* K_2CO_3 (0.32 g, 2.32 mmol) was added to a solution of 3-bromopropanol (0.29 g, 2.11 mmol) in dry DMF (30 mL) under N_2 atmosphere. The reaction mixture was heated at 130 °C and then a solution of thiophenol (0.26 g, 2.32 mmol) in 20 mL of dry DMF was added dropwise during a period of 3 h. The mixture was stirred at this temperature for 24 h. After evaporation of the solvent, the residue was taken up with EtOAc, washed with 2 N NaOH, and then with brine. The organic phase was dried (Na_2SO_4) and concentrated under vacuum. The residue was purified by column chromatography on silica gel (EtOAc/petroleum ether 2:8) to give 0.36 g (69%) of a yellow oil; IR (neat): 3356 (OH) cm^{-1}; ^1H NMR ($CDCl_3$): δ1.83–1.92 (m, 3H, $CH_2CH_2CH_2$ + O*H*), 3.03 (t, J = 7.15 Hz, 2H, CH_2SAr), 3.75 (t, J = 6.1 Hz, 2H, CH_2OH), 7.14–7.36 (m, 5H, ArS); ^{13}C NMR ($CDCl_3$): δ 30.5 (1C), 31.9 (1C), 61.6 (1C), 126.2 (1C), 129.1 (2C), 129.4 (2C), 136.5 (1C); GC/MS (70 eV) *m/z* (%) 168 (M^+, 10), 110 (100).

4.2. Enzymology

The compounds were screened for their activity and their species-specificity against *Ec*TS, *Ef*TS, and hTS. *Ec*TS, and hTS were purified as described [8]. *Ef*TS [14] was purified following the procedure used for *Ec*TS. Enzyme kinetics experiments were conducted by chromogenic assay under standard conditions [8,14]. The K_m values, by curve-fitting to hyperbolic curves, of *Ec*TS, *Ef*TS, and hTS for MTHF were, respectively, 5.8 μM, 13.6 μM, and 6.9 μM. These data represent the mean of triplicate measurements; in a typical study, the standard deviation of the data fell within ±20% of the mean. The apparent inhibition constant (K_i app, simply defined as K_i within the text) values were obtained from the linear least-squares fit of the residual activity as a function of inhibitor concentration, assuming a competitive inhibition [8]. In the inhibition assays, the reaction mixture was the same as in the TS standard assay. Stock solutions of each inhibitor were freshly prepared in dimethyl sulfoxide (DMSO) and stored at − 80 °C. In the reaction mixture, the concentration of DMSO never exceeded 5%. Each experiment was repeated at least three times and an individual measurement did not differ more than 20% from the mean.

4.3. Crystallization

Crystallization trials for *Ef*TS were performed using the vapor diffusion sitting drop method [56] at 297 K. Crystal Screen, Crystal Screen II and Greed Screen Ammonium Sulfate from Hampton Research were used for screening crystallization conditions. Drops consisting of 2 μL precipitant and 1 μL *Ef*TS solution (7.8 mg/mL in 25 mM KH_2PO_4/K_2HPO_4 pH 6.8, 40 mM dUMP, 1 mM EDTA) were equilibrated against 100 μL reservoir solution. After one month crystals were observed into a drop containing 3.2 M ammonium sulfate and 0.1 M HEPES buffer, pH 7.0 as precipitant solution. These crystals were ill-formed and provided a poor diffraction pattern when exposed to X-ray radiation, therefore we tried to improve the crystal ordering/quality by applying seeding techniques [56] The crystals obtained were crushed and seeding solutions were prepared by dilution with the successful precipitant solution (3.2 M ammonium sulfate and 0.1 M HEPES buffer, pH 7.0). 4 μL drops of a 2.5 mg/mL *Ef*TS solution (buffer 25 mM KH_2PO_4/K_2HPO_4 pH 6.8, 40 mM dUMP, 1 mM EDTA) were mixed with 2 μL of a precipitant solution containing 2.7 M ammonium sulfate and 0.1 M HEPES buffer, pH 7.0. Streak-seeding has been performed at different dilution of the seeding solution. Drops were allowed to equilibrate at room temperature over 0.6 mL precipitant solution in the well. Crystals suitable for diffraction appeared in 2–3 weeks into the drops in which a seeding solution diluted 1:100 was applied. Co-crystallization trials were performed also for the complexes *Ef*TS-inhibitor using the same precipitant solution identified in the previous screen for the enzyme (3.2 M ammonium sulfate and 0.1 M HEPES buffer, pH 7.0). Trials of co-crystallization were performed at 297 K using both the microbatch-under-oil crystallization technique [57,58] with a 1:1 mixture of paraffin and silicon oil (Hampton Research) as well as the sitting-drop vapor-diffusion method. Because of the low solubility in water, concentrated solutions of each inhibitor were prepared in DMSO. A 4 mM solution of each inhibitor in DMSO has been added in a 1:10 vol ratio to a 6.5 mg/mL *Ef*TS solution (buffer 25 mM KH_2PO_4/K_2HPO_4 pH 6.8, 40 mM dUMP, 1 mM EDTA). Drops have been prepared by mixing 2 μL of the *Ef*TS-inhibitor solution with 1 μL of a precipitant solution containing 3.2 M ammonium sulfate and 0.1 M HEPES buffer, pH 7.0. Crystals of *Ef*TS complexes with the library molecules have been finally obtained using the microbatch-under-oil crystallization technique. As it can be appreciated from the above description, the crystallization screen has been extremely difficult and was a cumbersome process, rich of failures. Under the microscope, all the crystals obtained presented defects like cracks and lines indicating internal disorder. Before data collection, crystals were transferred to a cryoprotectant solution containing 20% ethylene glycol and 80% precipitant solution (2.7 M ammonium sulfate and 0.1 M HEPES pH 7.0) and then flash frozen in liquid nitrogen.

4.4. Structure solution and refinement

About 70 crystals were screened for diffraction at the ESRF (European Synchrotron Radiation Facilities) beamline ID29-1. The data collection demonstrated that all crystals were characterized by severe splitting and suffered from radiation damage, with the diffraction pattern decaying after about 100 s of exposure to X-rays (0.5° oscillation images). Finally, we were able to obtain usable datasets referring to (*R*)-**2**, (*S*)-**12, 14** and **MTX** complexes. However, all of them were complete to a maximum of about 75–80%, but the missing data were randomly distributed in reciprocal space without jeopardizing the quality of the electron density maps [46]. Intensities were integrated using the program Mosflm [59] and scaled with the program Scala [60] or Aimless from the CCP4 Suite [61]. Data collection statistics are reported in Table S2 (see Supplementary Material). All *Ef*TS crystals belong to space group $P2_1$ with four *Ef*TS subunits in the asymmetric unit. The structures were solved by molecular replacement technique as implemented in the software MolRep [62] from the CCP4 Suite [61] using the crystal structure of *Lactobacillus casei* TS as model (PDB: 2TDM; 73% sequence homology). Because of the structural flexibility that characterize some domains of TS enzymes the *Lc*TS loop 82–144 was removed from the model. Molrep provided the correct solution that consists of a couple of *Ef*TS homodimers in the crystal asymmetric unit (A-B and C-D). The *Ef*TS molecule was manually rebuilt in the electron density maps. The whole polypeptide chain could be completely reconstructed only in the subunits were the inhibitor was bound. The unbound subunits presented disorder in the regions corresponding to residues 81–132 that were not clearly visible in the electron density maps and could be only partially built. The Fourier difference maps showed electron density interpretable with the presence of the inhibitor only for *Ef*TS-(*S*)-**12**, and *Ef*TS-MTX complexes. The final models were refined using the program Refmac5 [63] from the CCP4 Suite. Water molecules have been added using the program ArpWARP [64] and checked manually. The diffraction pattern of the crystals presented split reflections due to the lattice disordering as described above. This resulted in medium quality indicators of the refinement as shown in Table S2 (see Supplementary Material). Nevertheless, the electron density maps were quite well defined and could be confidently interpreted, as can be judged from the reported figures. The stereochemical quality of the final model was checked using the programs PROCHECK [65] and COOT [66]. The program COOT was also used for molecular modeling and to superimpose structures. Structural models were rendered using CCP4MG [67]. Atomic coordinates and structure factors for *Ef*TS-(*S*)-**12**, and *Ef*TS-MTX complexes have been deposited in the Protein Data Bank (PDB), www.rcsb.org, under the accession codes 4O7U and 5J7W, respectively.

Funding sources

The project has been supported by MIUR-PRIN2009 number 200925BPZ5_004.

Acknowledgment

We acknowledge the European Synchrotron Radiation Facility (ESRF), especially beamline ID29-1 for data collection facilities.

Abbreviations

DIAD	diisopropylazodicarboxylate
DMF	dimethylformamide
DMSO	dimethyl sulfoxide
dTMP	2′-deoxythymidine-5′-monophosphate
DTT	dithiothreitol
dUMP	2′-deoxyuridine-5′-monophosphate
*Ec*TS	*Escherichia coli* Thymidylate Synthase
EEDQ	2-ethoxy-1-ethoxycarbonyl-1,2-dihydroquinoline
EDTA	Ethylenediaminetetraacetic acid
*Ef*TS	*Enterococcus faecalis* Thymidylate Synthase
EtOH	Ethanol
Et3N	triethylamine
5-FTHF	5-formyl tetrahydrofolate
5-HMHF	5-hydroxymethyl-6-hydrofolate
hTS	Thymidylate Synthase
Ki	Inhibition Constant
*Lc*TS	*Lactobacillus casei* Thymidylate Synthase
MeOH	Methanol

MTHF	N5,N10-methylene tetrahydrofolate
NBS	N-bromosuccinimide; PEG, Poly(ethylene glycol)
SD	Small Domain
TFA	Trifluoroacetic acid
THF	Tetrahydrofuran
TMS	Trimethylsilane
TS	Thymidylate Synthase.

Appendix A. Supplementary data

Supplementary data related to this article can be found at http://dx.doi.org/10.1016/j.ejmech.2016.07.066.

References

[1] F.H. Kayser, Safety aspects of enterococci from the medical point of view, Int. J. Food Microb. 88 (2003) 255–262.

[2] T.J. Stout, D. Tondi, M. Rinaldi, D. Barlocco, P. Pecorari, D.V. Santi, I.D. Kuntz, R.M. Stroud, B.K. Shoichet, M.P. Costi, Structure-based design of inhibitors specific for bacterial thymidylate synthase, Biochemistry 38 (1999) 1607–1617.

[3] M.P. Costi, M. Rinaldi, D. Tondi, P. Pecorari, D. Barlocco, S. Ghelli, R.M. Stroud, D.V. Santi, T.J. Stout, C. Musiu, E.M. Marangiu, A. Pani, D. Congiu, G.A. Loi, P. La Colla, Phthalein derivatives as a new tool for selectivity in thymidylate synthase inhibition, J. Med. Chem. 42 (1999) 2112–2124.

[4] S. Ghelli, M. Rinaldi, D. Barlocco, A. Gelain, P. Pecorari, D. Tondi, G. Rastelli, M.P. Costi, Ortho-Halogen naphthaleins as specific inhibitors of Lactobacillus casei thymidylate synthase. Conformational properties and biological activity, Bioorg. Med. Chem. 11 (2003) 951–963.

[5] S. Calo, D. Tondi, A. Venturelli, S. Ferrari, P. Pecorari, M. Rinaldi, S. Ghelli, M.P. Costi, A step further in the discovery of phthalein derivatives as thymidylate synthase inhibitors, ARKIVOC (2004) 382–396.

[6] J.S. Finer-Moore, A.C. Anderson, R.H. O'Neil, M.P. Costi, S. Ferrari, J. Krucinski, R. Stroud, The structure of Cryptococcus neoformans thymidylate synthase suggests strategies for using target dynamics for species-specific inhibition, Acta Crystallogr. Sect. D. Biol. Crystallogr. D61 (2005) 1320–1334.

[7] M.P. Costi, A. Gelain, D. Barlocco, S. Ghelli, F. Soragni, F. Raniero, T. Rossi, A. Ruberto, C. Guillou, A. Cavazzuti, C. Casolari, S. Ferrari, Anti-bacterial agent discovery using thymidylate synthase bio-library screening, J. Med. Chem. 49 (2006) 5958–5968.

[8] S. Mangani, L. Cancian, R. Leone, C. Pozzi, S. Lazzari, R. Luciani, S. Ferrari, M.P. Costi, Identification of the binding modes of N-phenylphthalimides inhibiting bacterial thymidylate synthase through X-ray crystallography screening, J. Med. Chem. 54 (2011) 5454–5467.

[9] S. Ferrari, M. Ingrami, F. Soragni, R.C. Wade, M.P. Costi, Ligand-based discovery of N-(1,3-dioxo-1H,3H-benzo[de]isochromen-5-yl)-carboxamide and sulfonamide derivatives as thymidylate synthase a inhibitors, Bioorg. Med. Chem. Lett. 23 (2013) 663–668.

[10] S. Ferrari, S. Calò, R. Leone, R. Luciani, L. Costantino, S. Sammak, F. Di Pisa, C. Pozzi, S. Mangani, M.P. Costi, 2-Deoxyuridine 5′-monophosphate substrate displacement in thymidylate synthase through 6-hydroxy-2H-naphtho[1,8-bc]furan-2-one derivatives, J. Med. Chem. 56 (2013) 9356–9360.

[11] M.P. Costi, S. Ferrari, A. Venturelli, S. Calo, D. Tondi, D. Barlocco, Thymidylate synthase structure, function and implication in drug discovery, Curr. Med. Chem. 12 (2005) 2241–2258.

[12] C.W. Carreras, D.V. Santi, The catalytic mechanism and structure of thymidylate synthase, Ann. Rev. Biochem. 64 (1995) 721–762.

[13] E. Chu, M.A. Callender, M.P. Farrell, J.C. Schmitz, Thymidylate synthase inhibitors as anticancer agents: from bench to bedside, Cancer Chemother. Pharmacol. 52 (2003) S80–S89.

[14] C. Pozzi, S. Ferrari, D. Cortesi, R. Luciani, R.M. Stroud, A. Catalano, M.P. Costi, S. Mangani, The structure of Enterococcus faecalis thymidylate synthase provides clues about folate bacterial metabolism, Acta Crystallogr. D68 (2012) 1232–1241.

[15] A. Catalano, A. Carocci, M.S. Sinicropi, Mexiletine metabolites: a review, Curr. Med. Chem. 22 (2015) 1400–1413.

[16] A. Carocci, A. Catalano, C. Bruno, A. Lovece, M.G. Roselli, M.M. Cavalluzzi, F. De Santis, A. De Palma, M.R. Rusciano, M. Illario, C. Franchini, G. Lentini, *N*-(Phenoxyalkyl) amidesas MT_1 and MT_2ligands: antioxidantproperties and inhibition of Ca^{2+}/CaM-dependentkinase II, Bioorg. Med. Chem. 21 (2013) 847–851.

[17] J.F. Desaphy, A. Dipalma, T. Costanza, R. Carbonara, M.M. Di Nardo, A. Catalano, A. Carocci, G. Lentini, C. Franchini, D. Conte Camerino, Molecular insights into the local anesthetic receptor within voltage-gated sodium channels using hydroxylated analogs of mexiletine, Front. Pharmacol. 3 (2012) 1–12.

[18] A. Carocci, A. Catalano, A. Lovece, G. Lentini, A. Duranti, V. Lucini, M. Pannacci, F. Scaglione, C. Franchini, Design, synthesis, and pharmacological effects of structurally simple ligands for MT_1 and MT_2melatoninreceptors, Bioorg. Med. Chem. 18 (2010) 6496–6511.

[19] A. Carocci, G. Lentini, A. Catalano, M.M. Cavalluzzi, C. Bruno, M. Muraglia, N.A. Colabufo, N. Galeotti, F. Corbo, R. Matucci, C. Ghelardini, C. Franchini, Chiral aryloxyalkylamines: selective 5-$HT_{1B/1D}$ activation and analgesic activity, ChemMedChem. 5 (2010) 696–704.

[20] A. De Luca, S. Talon, M. De Bellis, J.F. Desaphy, C. Franchini, G. Lentini, A. Catalano, F. Corbo, V. Tortorella, D. Conte Camerino, Inhibition of skeletal muscle sodium currents by mexiletine analogues: specific hydrophobic interactions rather than lipophilia per se account for drug therapeutic profile, Naunyn-Schmied. Arch. Pharmacol. 367 (2003) 318–327.

[21] A. Catalano, A. Carocci, G. Fracchiolla, C. Franchini, G. Lentini, V. Tortorella, A. De Luca, M. De Bellis, J.F. Desaphy, D. Conte Camerino, Stereospecific synthesis of para-hydroxymexiletine and sodium canne blocking activity evaluation, Chirality 16 (2004) 72–78.

[22] A. Catalano, A. Carocci, M.M. Cavalluzzi, A. Di Mola, G. Lentini, A. Lovece, A. Dipalma, T. Costanza, J.F. Desaphy, D. Conte Camerino, C. Franchini, Hydroxylated analogs of mexiletine as tools for structural-requirements investigation of the sodium canne blocking activity, Arch. Pharm. Chem. Life Sci. 343 (2010) 325–332.

[23] A. Catalano, J.F. Desaphy, G. Lentini, A. Carocci, A. Di Mola, C. Bruno, R. Carbonara, A. De Palma, R. Budriesi, C. Ghelardini, M.G. Perrone, N.A. Colabufo, D. Conte Camerino, C. Franchini, Synthesis and toxicopharmacological evaluation of m-hydroxymexiletine, the first metabolite of mexiletine more potentthan the parent compound on voltage-gated sodium channels, J. Med. Chem. 55 (2012) 1418–1422.

[24] A. Catalano, R. Budriesi, C. Bruno, A. Di Mola, I. Defrenza, M.M. Cavalluzzi, M. Micucci, A. Carocci, F. Franchini, G. Lentini, Searching for new antiarrhythmic agents: evaluation of meta-hydroxymexiletine enantiomers, Eur. J. Med. Chem. 65 (2013) 511–516.

[25] A. Carocci, A. Catalano, F. Corbo, A. Duranti, R. Amoroso, C. Franchini, G. Lentini, V. Tortorella, Stereospecific synthesis of mexiletine and related compounds: Mitsunobu versus Williamson reaction, Tetrahedron Asymm. 11 (2000) 3619–3634.

[26] C. Bruno, M.M. Cavalluzzi, A. Carocci, A. Catalano, C. Franchini, G. Lentini, Capillary zone electrophoresis for separation and quantitative determination of mexiletine and its mainphase I metabolites, Drug Metab. Lett. 7 (2013) 52–57.

[27] R. Pascale, A. Carocci, A. Catalano, G. Lentini, A. Spagnoletta, M.M. Cavalluzzi, F. De Santis, A. De Palma, V. Scalera, C. Franchini, New *N*-(phenoxydecyl) phthalimide derivatives displaying potent inhibition activity towards alpha-glucosidase, Bioorg. Med. Chem. 18 (2010) 5903–5914.

[28] M. De Bellis, A. De Luca, F. Rana, M.M. Cavalluzzi, A. Catalano, C. Franchini, V. Tortorella, D. Conte Camerino, Evaluation of the pharmacological activity of the major mexiletine metabolites on skeletal muscle sodium currents, Br. J. Pharmacol. 149 (2006) 300–310.

[29] C. Lamanna, A. Catalano, A. Carocci, A. Di Mola, C. Franchini, V. Tortorella, M.S. Sinicropi, P.M.L. Vanderheyden, K.A. Watson, S. Sciabola, AT_1 receptor ligands: virtual-screening-based design with TOPP descriptors, synthesis, and biological evaluation of pyrrolidine derivatives, ChemMedChem. 2 (2007) 1298–1310.

[30] A. Duranti, C. Franchini, G. Lentini, F. Loiodice, V. Tortorella, A. De Luca, S. Pierno, D. Conte Camerino, 2000 Homologation of mexiletine alkyl chain and stereoselective blockade of skeletal muscle sodium channels, Eur. J. Med. Chem. 35 (2000) 147–156.

[31] C. Franchini, A. Carocci, A. Catalano, M.M. Cavalluzzi, F. Corbo, G. Lentini, A. Scilimati, P. Tortorella, D. Conte Camerino, A. De Luca, Optically active mexiletine analogues as stereoselective blockers of voltage-gated Na^+ channels, J. Med. Chem. 46 (2003) 5238–5248.

[32] M.M. Cavalluzzi, A. Catalano, C. Bruno, A. Lovece, A. Carocci, F. Corbo, C. Franchini, G. Lentini, V. Tortorella, Synthesis of (R)-, (S)-, and (RS)-hydroxymethylmexiletine, one of the major metabolites of mexiletine, Tetrahedron Asymm. 18 (2007) 2409–2417.

[33] M. De Bellis, A. De Luca, J.F. Desaphy, J. Heiny, A. Kennedy, A. Carocci, M.M. Cavalluzzi, G. Lentini, C. Franchini, D. Conte Camerino, Combined modifications of mexiletine pharmacophores for new lead blockers of Nav1.4 channels, Biophys. J. 104 (2013) 344–354.

[34] A. Catalano, A. Carocci, I. Defrenza, M. Muraglia, A. Carrieri, F. Van Bambeke, A. Rosato, F. Corbo, F. Franchini, 2-Aminobenzothiazole derivatives: search for new antifungal agents, Eur. J. Med. Chem. 64 (2013) 357–364.

[35] A. Carocci, A. Catalano, C. Bruno, G. Lentini, C. Franchini, M. De Bellis, A. De Luca, D. Conte Camerino, Synthesis and in vitro sodium channel blocking activity evaluation of novel homochiral mexiletine analogs, Chirality 22 (2010) 299–307.

[36] A. Catalano, A. Carocci, F. Corbo, C. Franchini, M. Muraglia, A. Scilimati, M. De Bellis, A. De Luca, D. Conte Camerino, M.S. Sinicropi, V. Tortorella, Constrained analogues of tocainide as potent skeletal muscle sodium channel blockers towards the development of antimyotonic agents, Eur. J. Med. Chem. 43 (2008) 2535–2540.

[37] A. Catalano, A. Carocci, G. Lentini, I. Defrenza, C. Bruno, C. Franchini, Stereospecific synthesis of m-hydroxymexiletine enantiomers, Drug. Metab. Lett. 6 (2012) 182–186.

[38] A. Catalano, A. Carocci, G. Lentini, I. Defrenza, M.M. Cavalluzzi, C. Franchini, An improved synthesis of m-hydroxymexiletine, a potent mexiletine metabolite, Drug. Metab. Lett. 6 (2012) 124–128.

[39] F. Maley, J. Pedersen-Lane, L. Changchien, Complete restoration of activity to inactive mutants of Escherichia coli thymidylate synthase: evidence that E. coli thymidylate synthase is a half-the-sites activity enzyme, Biochemistry 34

(1995) 1469–1474.
[40] A.C. Anderson, R.H. O'Neil, W.L. DeLano, R.M. Stroud, The structural mechanism for half-the-sites reactivity in an enzyme, thymidylate synthase, involves a relay of changes between subunits, Biochemistry 38 (1999) 13829–13836.
[41] D.L. Birdsall, J. Finer-Moore, R.M. Stroud, The only active mutant of thymidylate synthase D169, a residue far from the site of methyl transfer, demonstrates the exquisite nature of enzyme specificity, Protein Eng. 16 (2003) 229–240.
[42] S. Chen, D.H. Shin, R. Pufan, R. Kim, S.H. Kim, Crystal structure of methenyltetrahydrofolate synthetase from Mycoplasma pneumoniae (GI: 13508087) at 2.2 A resolution, Proteins 56 (2004) 839–843 (PDB: 1U3G).
[43] B.K. Shoichet, R.M. Stroud, D.V. Santi, I.D. Kuntz, K.M. Perry, Structure-based discovery of inhibitors of thymidylate synthase, Science 259 (1993) 1445–1450.
[44] Z. Wang, T. Abeysinghe, J.S. Finer-Moore, R.M. Stroud, A. Kohen, A remote mutation affects the hydride transfer by disrupting concerted protein motions in thymidylate synthase, J. Am. Chem. Soc. 134 (2012) 17722–17730.
[45] A. Tochowicz, S. Dalziel, O. Eidam, J.D. O'Connell, S. Griner, J.S. Finer-Moore, R.M. Stroud, Development and binding mode assessment of N-[4-[2-propyn-1-yl[(6S)-4,6,7,8-tetrahydro-2-(hydroxymethyl)-4-oxo-3H-cyclopenta[g]quinazolin-6-yl]amino]benzoyl]-l-γ-glutamyl-D-glutamic acid (BGC 945), a novel thymidylate synthase inhibitor that targets tumor cells, J. Med. Chem. 56 (2013) 5446–5455.
[46] Z. Dauter, Data-collection strategies, Acta Crystallogr. D. Biol. Crystallogr. 55 (1999) 1703–1717.
[47] A. Catalano, A. Carocci, A. Di Mola, P.M.L. Vanderheyden, C. Franchini, 1-Pentanoyl-N-{[2′-(1H-tetrazol-5-yl)biphenyl-4-yl]methyl}-pyrrolidine-2-carboxamide: investigation of structural variations, Arch. Pharm. Chem. Life Sci. 344 (2011) 617–626.
[48] C. Bruno, A. Carocci, A. Catalano, M.M. Cavalluzzi, F. Corbo, C. Franchini, G. Lentini, V. Tortorella, Facile, alternative route to lubeluzole, itsenantiomer and the racemate, Chirality 18 (2006) 227–231.
[49] M. Muraglia, M. De Bellis, A. Catalano, A. Carocci, C. Franchini, A. Carrieri, C. Fortugno, C. Bertucci, J.F. Desaphy, A. De Luca, D. Conte Camerino, F. Corbo, N-aryl-2,6-dimethylbenzamides, a new generation of tocainide analogues as blockers of skeletal muscle voltage-gated sodium channels, J. Med. Chem. 57 (2014) 2589–2600.
[50] W.V. Murray, M. P. Wacther, Substituted N-biphenylyl lactams, Patent WO 1993/5182288.
[51] M.V. Khedkar, S.R. Khan, K.P. Dhake, B.M. Bhanage, Carbonylative cyclization of o-halobenzoic acids for synthesis of N-substituted phthalimides using polymer-supported palladium-N-heterocyclic carbene as an efficient, heterogeneous, and reusable catalyst, Synthesis 44 (2012) 2623–2629.
[52] H. Takahashi, S. Sou, R. Yamasaki, M. Sodeoka, Y. Hashimoto, α-Glucosidase inhibitors with a phthalimide skeleton: structure activity relationship study, Chem. Pharm. Bull. 48 (2000) 1974–1983.
[53] N. Aguilar, A. Moyano, M.A. Pericàs, A. Riera, A mild, selective, PyBOP mediated procedure for the conversion of primary amines into phthalimides, Synthesis (1998) 313–316.
[54] A.A. Bahajaj, M.H. Moore, J.M. Vernon, Asymmetric synthesis of spiro 2-pyrrolidin-5-ones, 2-piperidin-6-ones and 1-isoindolin-3-ones. Part 1: N-Acyliminium ion cyclisations with an internal arene nucleophile, Tetrahedron 60 (2004) 1235–1246.
[55] R.A. Glennon, N.A. Naiman, M.E. Pierson, J.D. Smith, A.M. Ismaiel, M. Titeler, R.A. Lyon, *N*-(Phthalimidoalkyl) derivatives of serotonergic agents: a common interaction at 5-HT_{1A} serotonin binding sites? J. Med. Chem. 32 (1989) 1921–1926.
[56] M. Benvenuti, S. Mangani, Crystallization of soluble proteins in vapor diffusion for x-ray crystallography, Nat. Protoc. 2 (2007) 1633–1651.
[57] N.E. Chayen, A novel technique for containerless protein crystallization, Protein Eng. 9 (1996) 927–929.
[58] N.E. Chayen, The role of oil in macromolecular crystallization, Structure 5 (1997) 1269–1274.
[59] A.G. Leslie, The integration of macromolecular diffraction data, Acta Crystallogr. D. Biol. Crystallogr. 62 (2006) 48–57.
[60] P. Evans, Scaling and assessment of data quality, Acta Crystallogr. D. Biol. Crystallogr. 62 (2006) 72–82.
[61] M.D. Winn, C.C. Ballard, K.D. Cowtan, E.J. Dodson, P. Emsley, P.R. Evans, R.M. Keegan, E.B. Krissinel, A.G. Leslie, A. McCoy, S.J. McNicholas, G.N. Murshudov, N.S. Pannu, E.A. Potterton, H.R. Powell, R.J. Read, A. Vagin, K.S. Wilson, Overview of theCCP4 suite and current developments, Acta Crystallogr. D. Biol. Crystallogr. 67 (2011) 235–242.
[62] A. Vagin, A. Teplyakov, Molecular replacement with MOLREP, Acta Crystallogr. D. Biol. Crystallogr. 66 (2010) 22–25.
[63] G.N. Murshudov, A.A. Vagin, E.J. Dodson, Refinement of macromolecular structures by the maximum-likelihood method, Acta Crystallogr. D53 (1997) 240–255.
[64] R.J. Morris, A. Perrakis, V.S. Lamzin, ARP/wARP and automatic interpretation of protein electron density maps, Methods Enzymol. 374 (2003) 229–244.
[65] R.A. Laskowski, M.W. MacArthur, D.S. Moss, J.M. Thornton, PROCHECK: a program to check the stereochemical quality of protein structures, J. Appl. Crystallogr. 26 (1993) 283–291.
[66] P. Emsley, B. Lohkamp, W.G. Scott, K. Cowtan, Features and development of coot, Acta Crystallogr. D. Biol. Crystallogr. 66 (2010) 486–501.
[67] S. McNicholas, E. Potterton, K.S. Wilson, M.E.M. Noble, Presenting your structures: the CCP4mg molecular-graphics software, Acta Cryst. D67 (2011) 386–394.